REPORT OF ACTIVE FAULT MAPPING IN BANGLADESH : PALEO-SEISMOLOGICAL STUDY OF THE DAUKI FAULT AND THE INDIAN-BURMAN PLATE BOUNDARY FAULT

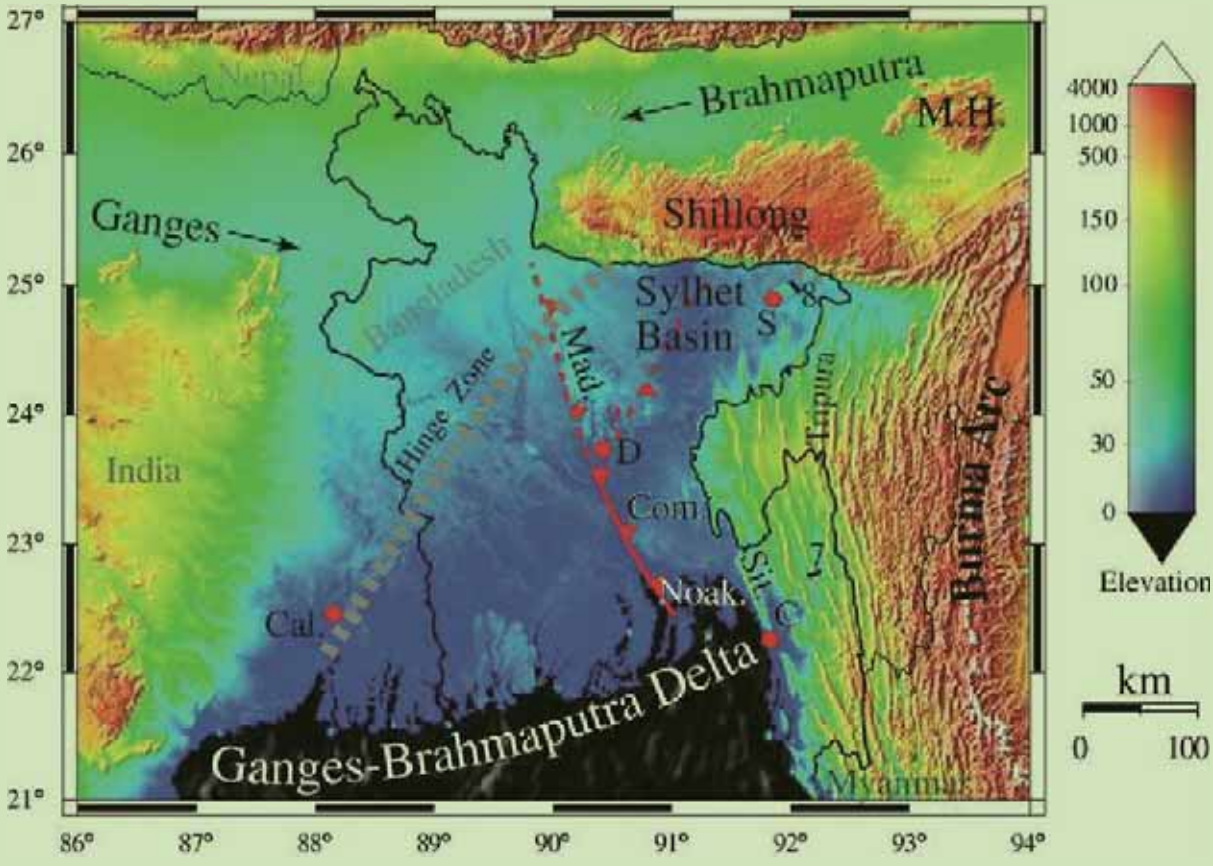

Printing supported by:

Comprehensive Disaster Management Programme (CDMP II)
Ministry of Disaster Management and Relief

UKaid from the British people
European Union
NORWEGIAN EMBASSY
SWEDEN
Australian AID
UNDP
Empowered lives. Resilient nations.

Report of active fault mapping in Bangladesh : Paleo-seismological study of the Dauki fault and the Indian-Burman plate boundary fault

March 2013

Michio Morino
International Short-Term Expert of UNDP

A. S. M. Maksud Kamal
Dhaka University

Reshad Md. Ekram Ali, Animesh Talukder, and MD. Mahmood Hassain Khan
Geological Survey of Bangladesh

Contents

Abstract

We carried out the Tectonic-geomorphic investigation and trench investigation on the Dauki fault and the Tripura segment of the Indian-Burman plate boundary fault, which are major active structures in Bangladesh, and evaluated the seismic risk of earthquake occurrence.

Dauki fault

A back-tilted lower terrace was identified at Jaflong, the north of Sylhet and the trench investigation was performed at the southern edge of the terrace. The flexure structure was identified in the trench, while an active fault was concealed. The timing of the seismic event that has created the flexure structure is inferred to be AD 880-1020 (Morino and Kamal, 2012). The time of this seismic event corresponds to that of the paleo-liquefaction which was identified on the north of the Shillong Plateau. Most of the paleo-liquefactions on the Shillong Plateau may have been created by the rupture of the Dauki fault, since its fault plane extends beneath the Shillong Plateau. The rupture of the Dauki fault in AD 1548 is identified at Gabrakhari trench site, and it is thought that the 1897 Great Assam earthquake also has been caused by the rupture of the Dauki fault from the hat-shaped intensity distribution. The time of the latest event of the Dauki fault is AD 1897, and its recurrence interval is 350-650 years. The probability of the earthquake occurrence within 50 years is relatively high with 7.7 %.

Tripura segment

The location of the Tripura segment is in debate. We think that the Tripura segment follows the western margin of the Chittagong-Tripura Fold Belt (CTFB) from GPS data and the tectonic-geomorphic investigation. However, no active fault was identified in the trench, although the tectonic-geomorphology is clear. The fault scarp or warping scarp may be eroded. The crater and the lateral flow were identified at Shahzibazar and the Comilla Hill, respectively. These events indicate that this region has been shaken by a large earthquake in 1120-400 BC. According to GPS data, the slip rate of the Tripura segment on the western margin of the CTFB is inferred to be 5 mm/year. Its recurrence interval may be as long as several thousand years, since the slip rate is small. The time of the latest seismic event of the Tripura segment is thought to be 1120-400 BC. The 50 years probability of earthquake occurrence is inferred to be 5.1 %.

Arakan segment

According to Shishikura et al. (2009), the recurrence interval of the 1762-type earthquake is 900 years. However, another-type earthquakes, the magnitude of which is smaller than the

1762-type, may occur between the 1762-type large earthquakes (EOS draft report). In this case, 50 years probability of earthquake occurrence is high over 13.4 %.

Active faults within the CTFB

The 1822 earthquake and the 1918 Srimongal earthquake are thought to have been caused by the rupture of active faults within the CTFB. If these are estimated as floating earthquakes on the Tripura segment, the recurrence interval is ~100 years, and 50 years probability is high with 64.9 %.

Issues in future

The issues in future on the paleo-seismological studies of Bangladesh are as follows:

There is no definitive evidence that the Dauki fault has ruptured in 1897. The tectonic -geomorphic investigation and trench investigation in the central part of the Dauki fault are necessary.

There is another suggestion that the Tripura segment passes around the mouth of Padma River (Steckler et al., 2008), while we think that the Tripura segment follows the western margin of the CTFB. The deep seismic reflection survey from the western margin of the CTFB to the Padma River is desirable. It is important to reveal the active structure across this region. Also the additional trench investigation should be tried at Kasba and Comilla Hill after the shallow seismic reflection survey.

1. Introduction

The tectonic-geomorphic investigation and paleo-seismological study based on trench investigation were performed for total 8 months of 3 months as CDMP-1 and 5 months as CDMP-2. The Dauki fault and the Tripura segment of the Indian-Burman plate-boundary fault were mainly targeted as trench investigation. Only tectonic geomorphic investigation was performed along the Madhupur blind fault and active faults within the Chittagong- Tripura Fault Belt (CTFB). The shallow seismic reflection survey was planned to select trench sites in CDMP-2. However, we could not refer the result, since the survey was delayed.

The important papers after Steckler et al. (2008) and Maurin and Rangin (2009) on the Indian-Burman plate-boundary fault were published during the practice of CDMP-1 and CDMP 2. Also the papers on the historical earthquakes in and around Bangladesh were published by Martin and Szeliga (2010) and Szeliga et al. (2010). Yu and Sieh submitted the EOS draft report of the active tectonics in and around Bangladesh to CDMP on July 2012. Dr. S. H. Akhter offered the unpublished GPS data in Bangladesh and its interpretation to us. We prepared the report referring EOS draft report and unpublished data after Dr. S. H. Akhter.

2. Active faults and historical earthquakes in Bangladesh

2.1 Active faults

Bangladesh stands on the northeastern corner of the Indian plate. There are two major structures relative to the plate boundary, namely the Dauki fault and the Indian-Burman plate boundary fault. The strike of the Dauki fault is parallel to the Himalayan Front fault, so this fault is thought to be related to the Indian-Eurasian plate boundary fault. A number of active faults is suggested within the Chittagong-Tripura Fold Belt, and the Madhupur blind fault is inferred on the western margin of the Madhupur Tract.

1) Dauki fault

The Himalayan Front Fault (HFF) as a mega-thrust is developed on the collision boundary between the Indian and Eurasian plates (Nakata, 1975, 1989). The Shillong Plateau stands on the south of the HFF, and the Dauki fault, which is a north-dipping reverse fault, passes on the southern margin of the Shillong Plateau (Fig. 1). The Shillong Plateau is composed of bedrocks of the Indian shield, which was uplifted by the activity of the Dauki fault with ~2000 m high. The Dauki fault is thought to be an active fault related to the collision boundary, since its strike is parallel to the HSS, while it is an intra-plate active fault within the Indian plate.

The southern part of the Shillong Plateau shows a positive gravity anomaly over + 20 mgal, while the Alluvial Plain on the south of the Shillong Plateau shows a remarkable negative gravity anomaly over −80 mgal (Rahman et al., 1990; Narula et al., 2000). The gravity anomaly contours are closely arranged with E-W direction on the southern margin of the Shillong Plateau. The Shillong Plateau shows asymmetrical topographic profile with the southern steep slope and the northern gentle slope. These gravity anomaly data and geomorphic features strongly suggest the presence of the Dauki fault (Morino et al., 2011).

2) Indian−Burman plate boundary fault

The slip partitioning is inferred on the eastern margin of the Indian plate due to its oblique convergence to the Eurasian plate. The mega-thrust along the subduction zone and the Sagaing fault as a right lateral fault are developed on both the western and eastern sides of

accretionary prisms, respectively. The N-S long region between these faults behaves as a micro plate and is called the Burman plate as a part of the Eurasian plate, while it consists of accretionary prisms on the hanging wall of the mega-thrust. The fold belt with the N-S axis is characteristic of the Burman plate. The western part of the accretionary prisms is younger and called Chittagong-Tripura Fold Belt (CTFB).

The plate boundary fault from off Myanmar to off Chittagong is the northern extension of the rupture area which has caused the 2004 Mw 9.2 off Sumatra earthquake (Fig. 2a). The 1762 earthquake has occurred in this region and accompanied the tsunami in the river near Dhaka (Steckler et al., 2008).

It is thought that the plate boundary extends to the north of off Chittagong and it comprises a different segment from that of off Myanmar to off Chittagong, since this segment has not ruptured in 1762. We call the former Tripura segment and the latter Arakan segment in this report (Fig. 1). The Tripura segment has a different faulting history and recurrence interval from the Arakan segment.

The detailed location of the plate boundary fault in and around Bangladesh is in debate. Steckler et al. (2008) suggest that the Comilla Tract is an uplifted terrace, and the buried front of a mega-thrust reaches to the mouth of Padma River (Figs. 2b and 2c). Furthermore, the Madhupur blind fault is estimated to be the northwestern extension of the Tripura segment (Fig. 2b). Maurin and Rangin (2009) suggested that the Chittagong Coastal Fault is considered to be the plate boundary fault, which is a thick-skinned right lateral fault, on the western margin of the Chittagong-Tripura Fold Belt (CTFB), and the deformation front is inferred on the west of the Comilla Tract (Figs. 3a and 3b).

Based on the tectonic-geomorphic investigation, we suggest that the Tripura segment passes along the western margin of the CTFB, and the deformation front is located around the mouth of Padma River (Fig. 1), since the deep seismic reflection survey is indicative of the deformation front more west (Fig. 3a; Maurin and Rangin, 2009). The fault traces of the Tripura segment were suggested from our tectonic-geomorphic investigation. The fault traces of the Arakan segment was extracted from the Chittagong Coastal Fault after Maurin and Rangin (2009).

The Comilla uplifted terrace is an interesting suggestion. However, the terrace extends 100 km wide. It is suspicious that a 100 km-wide terrace was uplifted by the activity of the mega-thrust.

3) Active faults within Chittagong-Tripura Fault Belt

Most of active faults within Chittagong-Tripura Fold Belt (CTFB) is thought to be

secondary faults and deformations related to the rupture of the Tripura segment. However, a part of these faults may generate large earthquakes separately from the plate boundary fault like the 1918 Srimongal earthquake. However, it is difficult to separate active structures from the secondary structures.

If the tectonic-geomorphology is identified on the younger surfaces in the Late Quaternary time, active structures will be distinguished from the secondary structures.

4) Madhupur blind fault

The Madhupur blind fault is inferred on the western margin of the Madhupur Tract, northwest of Dhaka (Fig. 1). The fault is considered as an important structure for the seismic hazard assessment of Dhaka, the capital of Bangladesh, although there is no definitive evidence for its presence.

The Madhupur Tract is characterized by red-color residual deposits on the surface (Alam et al., 1990). It is thought that the alluvium in the Quaternary time was uplifted and the soil on the surface was changed into red-color clay by weathering. The surface of Madhupur Tract is tilted to the east. The straight low scarps with NW-SE direction are recognized on the western margin of the Madhupur Tract (Fig. 1). The low scarps seem to be erosional. However, it is sure that the Madhupur Tract is uplifted and tilted to the east by the faulting. The flexural scarps, which have been uplifted by the activity of the Madhupur blind fault, may be eroded and shifted to the east.

Steckler et al. (2008) consider the Madhpur blind fault as the northwestern extension of the Tripura segment. However, the Madhupur blind fault is thought to be another intra-plate fault.

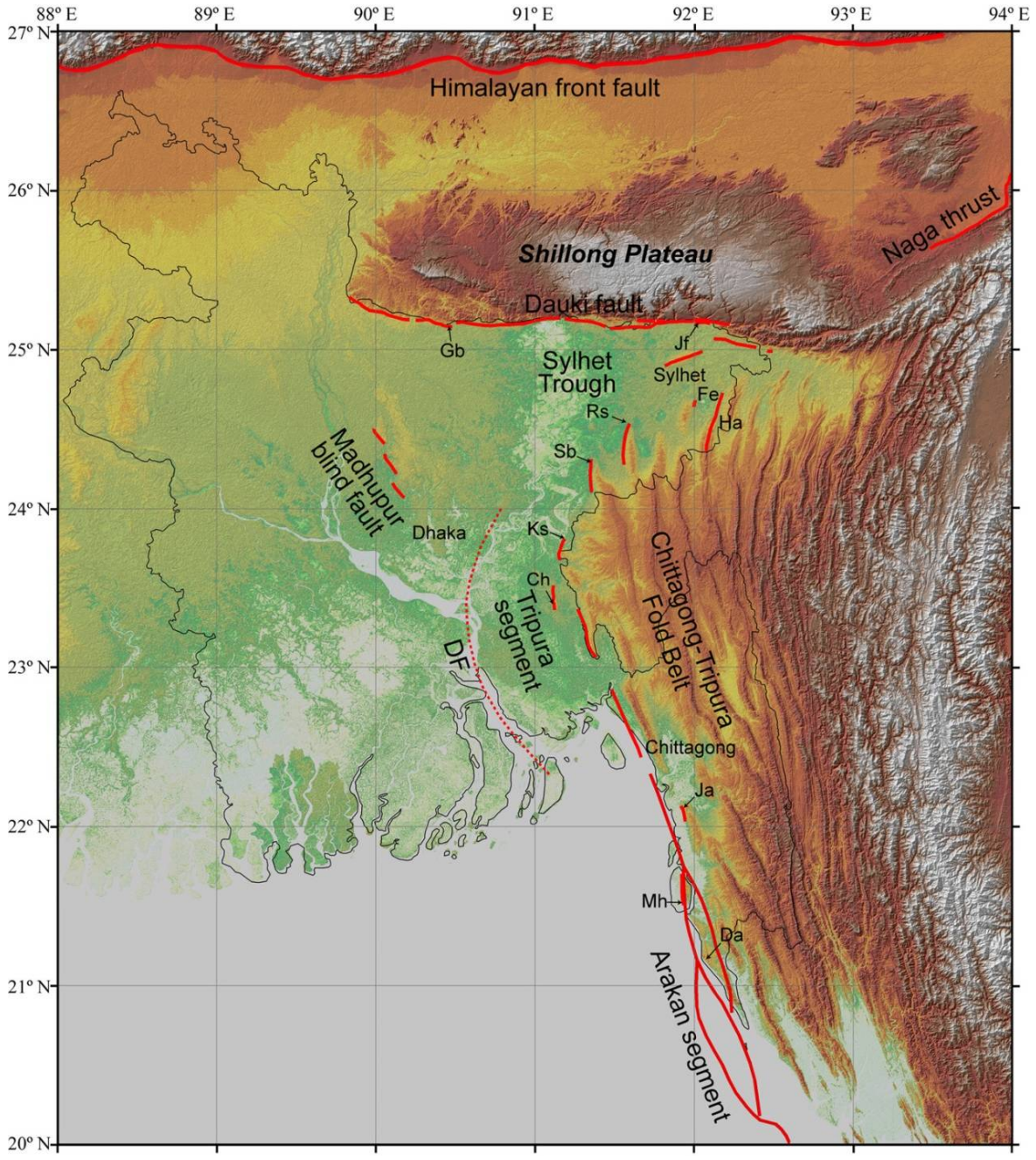

Figure 1. Active faults in and around Bangladesh. The dashed line represents a deformation front (DF). The fault traces of the Arakan segment are extracted from the fault traces of Chittagong Coastal Fault after Maurin and Rangin (2009). See Fig. 4. Gb: Gabrakhari, Jf: Jaflong, Fe: Fenchunganj, Ha: Hararganj. Rs: Rashidpur, Sb: Shahzibazar, Ks: Kasba, Ch: Comilla hill, Ja: Jaldi, Mh: Maheshkhali, Da: Dakshin Nila

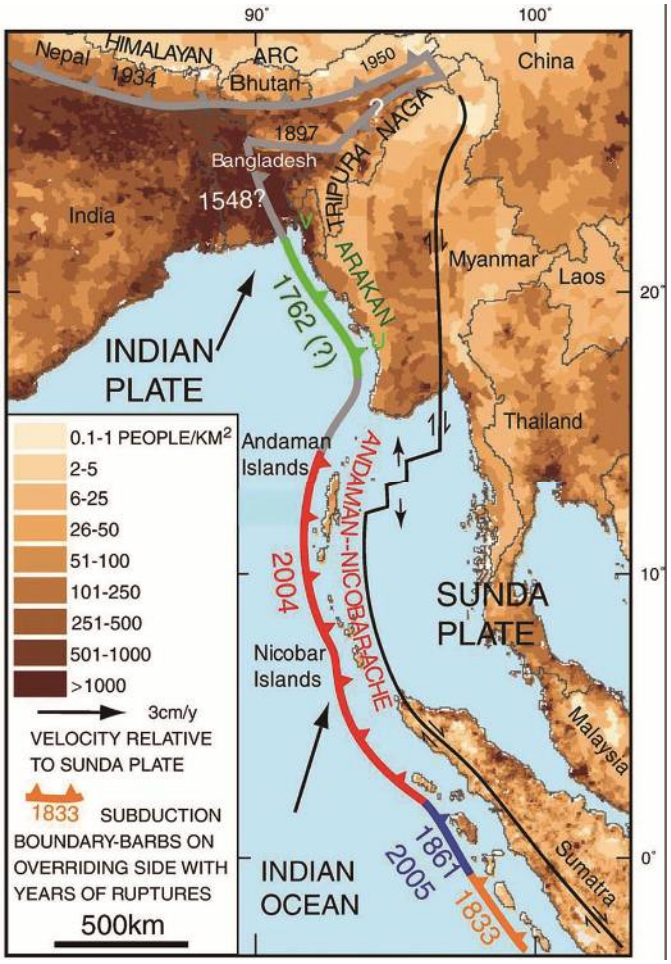

Figure 2a. Indian-Burman plate-boundary fault after Steckler et al. (2008)

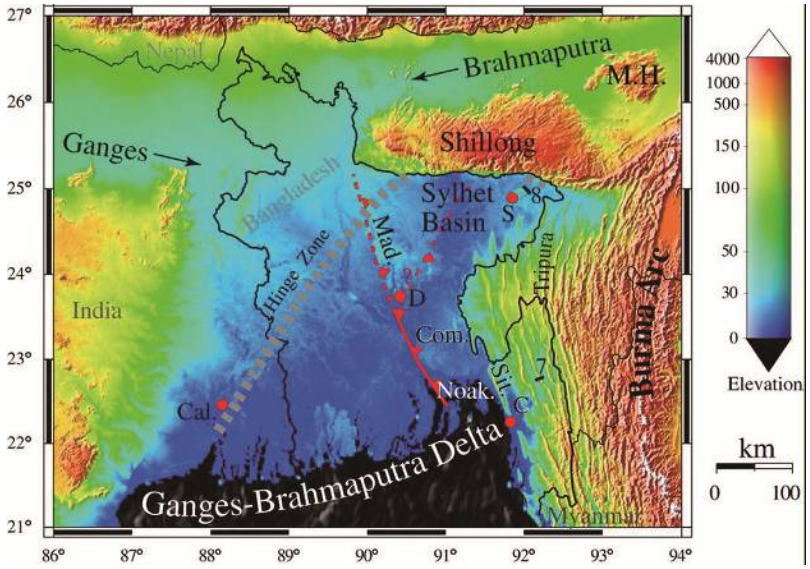

Figure 2b. The detailed location of the Tripura segment of the Indian-Burman plate-boundary fault after Steckler et al. (2008). Com: Comilla Tract (uplifted terrace), D: Dhaka, Mad: Madhupur Tract.

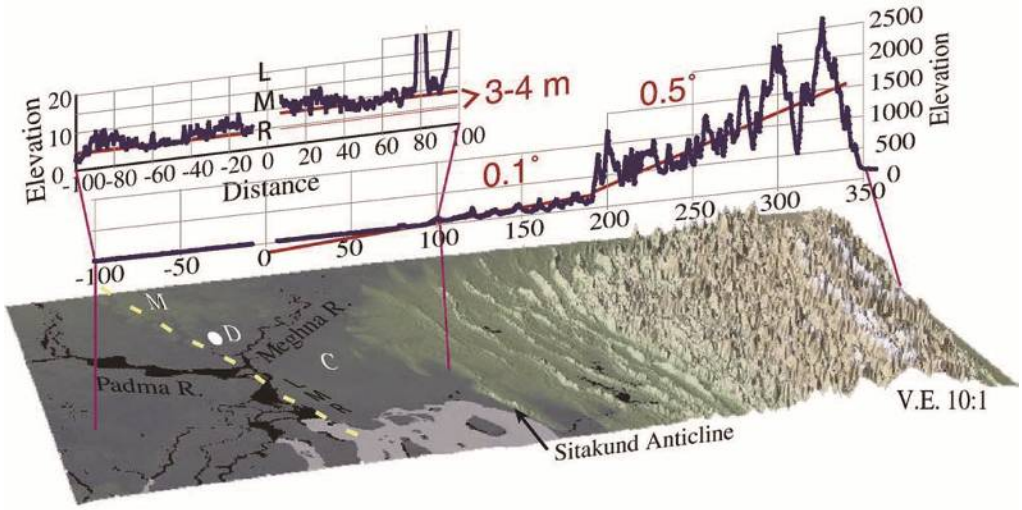

Figure 2c. Topographic profile across the uplifted Comilla terrace after Steckler et al. (2008)

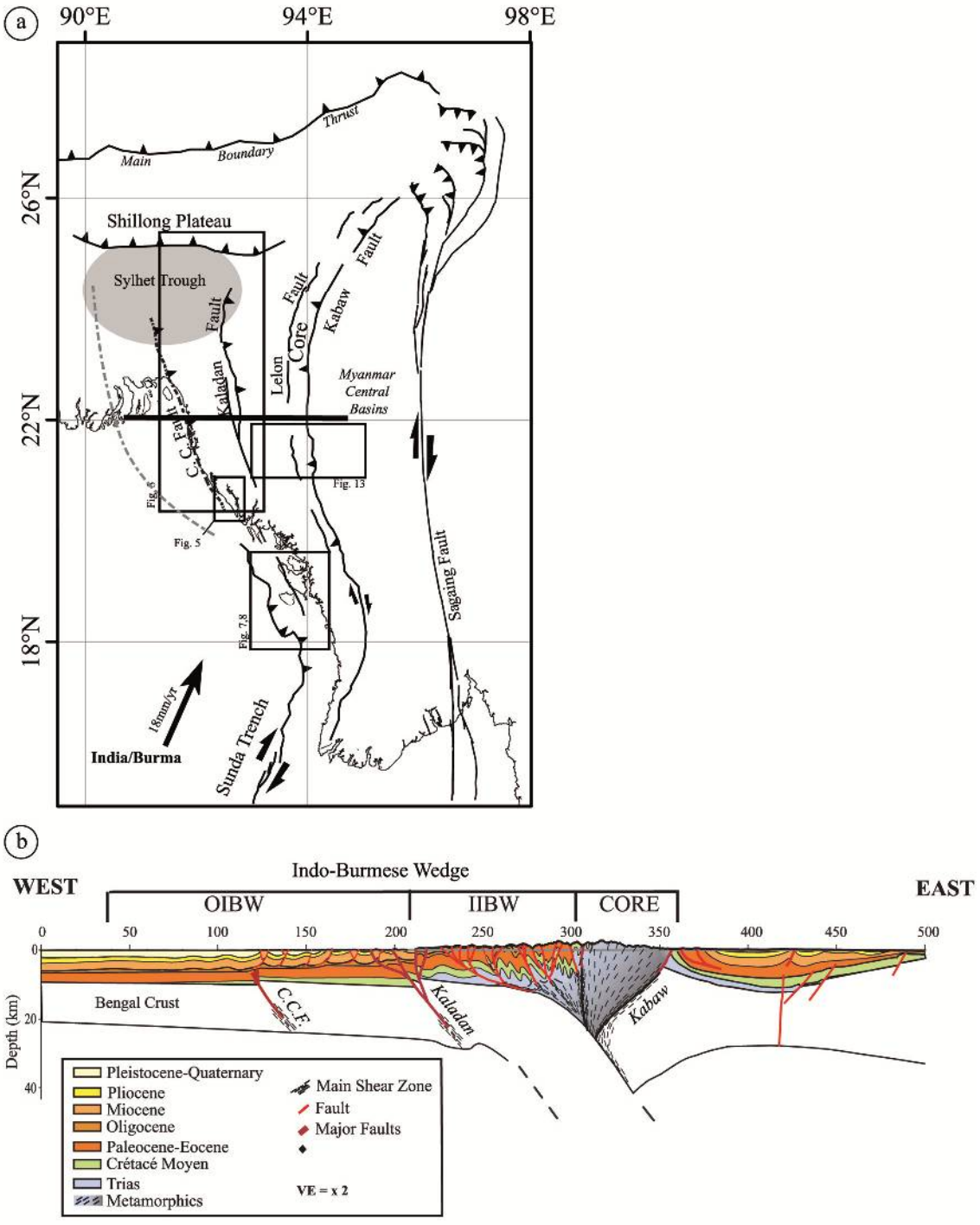

Figure 3. (a): Chittagong Coastal Fault (C. C. Fault) and deformation front (gray dashed line) after Maurin and Rangin (2009), (b): E-W geological cross section. The location is shown as a thick line in Fig. 3a.

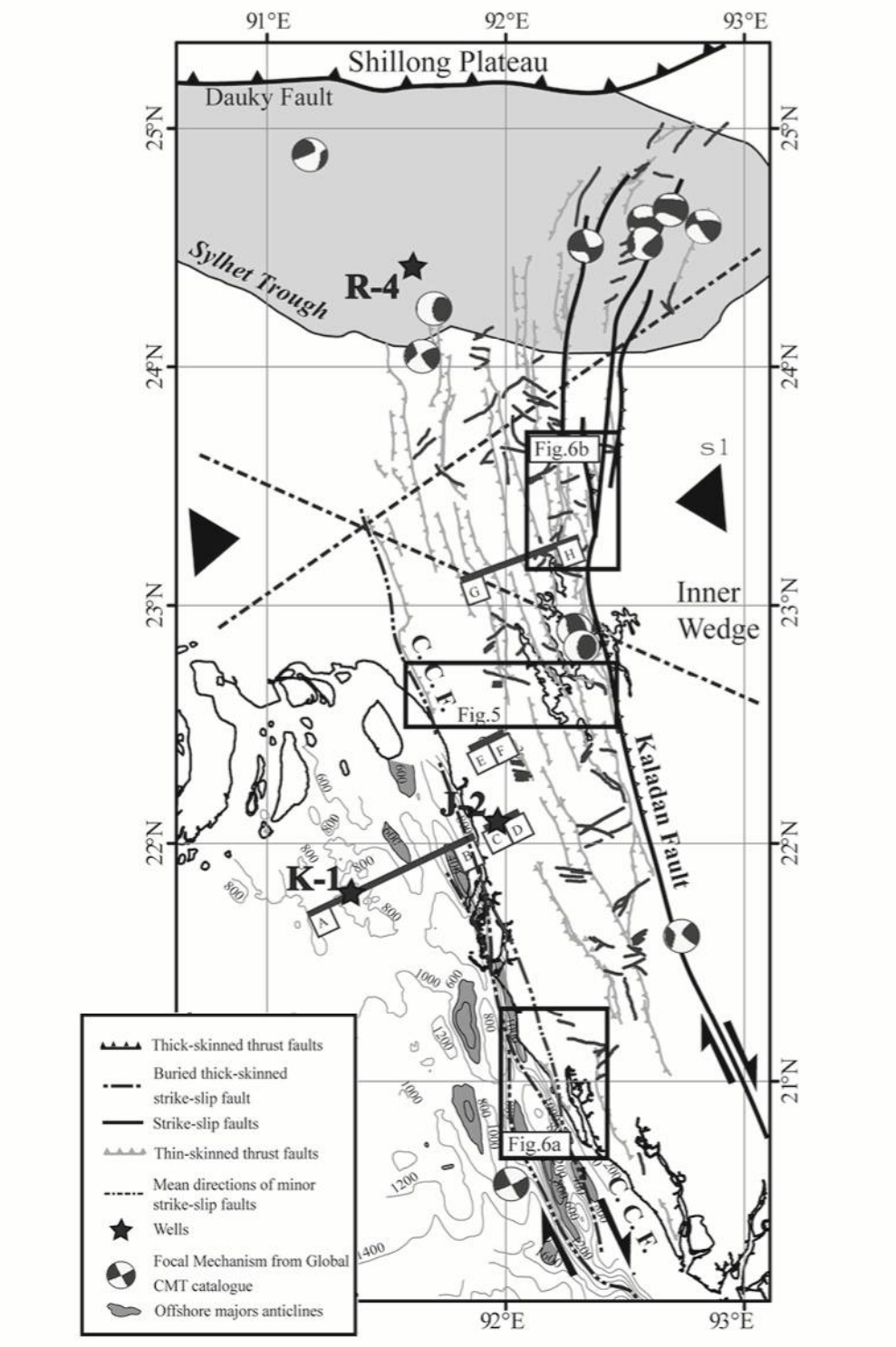

Figure 4. The detailed location of Chittagong Coastal Fault (C. C. F.). The thick black lines represent the lines of deep seismic reflection survey.

2.2 Historical earthquakes

Large historical earthquakes since the 1762 earthquake in the catalogue after Szeliga et al. (2010) are shown in Fig. 4. Major historical earthquakes in and around Bangladesh are shown in Table 1. These figure and table are extracted from EOS draft report after Yu and Sieh. In this section, the details of historical earthquakes are not discussed, and only important historical earthquakes for paleo-seismological study are mentioned.

1) 1548 earthquake

The 1548 earthquake, that Sylhet and Chittagong have suffered severe damages from, is a first-recorded large historical earthquake in Bangladesh (website: Banglapedia Earthquake). Bilham and Hough (2006) and Steckler et al. (2008) considered that the Tripura segment of the Indian and Burman plate boundary fault is a seismic source of the 1548 earthquake from the damage distribution. However, as mentioned by Steckler et al. (2008), there is no historical record that Dhaka or nearby Sonargaon, the capital at the time, has suffered damages from the 1548 earthquake. If the Tripura segment is a seismic source of this earthquake, Dhaka must have received severe damages. Furthermore, there is no paleo-seismological evidence that the Tripura segment has ruptured in 1548.

Morino et al. (2011) suggested that the Dauki fault has ruptured in 16th century and this seismic event corresponds to the 1548 earthquake. According to paleo-liquefaction studies in the north of the Shillong Plateau (Sukhija et al., 1999; Rajendran et al., 2004), the paleo-liquefaction in AD 1450-1650 is reported. The paleo-liquefaction on the north of the Shillong Plateau may have been created by the rupture of the Dauki fault in 1548, since the Dauki fault dips beneath the Shillong Plateau at an angle of ~45°.

2) 1762 Arakan earthquake

The western coastal areas and islands from Myanmar to Chittagong were widely uplifted by the rupture of the Arakan segment during the 1762 earthquake. The extensive flooding is reported in the coast of Noakhali, and in the river, south of Dhaka, boats were overturned and 500 people died during the 1762 earthquake (Steckler et al., 2008). Probably these damages are ascribed to the tsunami. The remarkable coastal uplifts are documented in the Islands off Myanmar. The uplifts amount to 4 m in Ramree Island, 3-7 m in Cheduba Island, and 3 m in Faul Island (Halsted, 1843; Aung et al., 2008). Aung et al. (2008) studied the uplifted marine terraces in West Phayonkan Island, off Myanmar, and revealed that the latest seismic event

that uplifted the coast is dated to AD 1762. Shishikura et al. (2009) inferred that the recurrence period of the 1762-type large earthquake is ~900 years.

We had a preliminary field survey with Dr. Shishikura along the coast from Cox' Bazar to Teknaf and confirmed several uplifted marine terraces. It is inferred that the uplifted marine terraces are developed along the coast from Myanmar to Chittagong.

3) 1897 Great Assam earthquake

The 1897 earthquake is inferred to be caused by the rupture of the Dauki fault from the hat-shaped strong intensity distribution (Oldham, 1899). However, there is no surface rupture in 1897 along the Dauki fault, while the paleo-liquefaction during the 1897 earthquake is confirmed at Gabrakhari and Awlatory (Morino et al., 2011). The rupture of the Dauki fault in 1897 may not have reached the surface around Gabrakahri.

Bilham and England (2001) and Rajendran et al. (2004) suggested the south-dipping reverse fault on the north of the Shillong Plateau as the seismic source of the 1897 earthquake. However, no tectonic-geomorphology is identified in this area.

4) 1822 and 1918 Srimongal earthquakes

The epicenters of these earthquakes are located near the Chittagong-Tripura Fold Belt (CTFB), so the seismic sources are thought to be active faults within the CTFB. It is important to reveal the seismic sources of these earthquakes in order to estimate the activity of active faults within the CTFB.

5) 1885 Bengal earthquake

The epicenter of the 1885 earthquake is inferred near Manikganj, 50 km northwest of Dhaka. It is believed that the Madhupur blind fault is a seismic source of this earthquake (website: Earthquakes of Dhaka). Although there is no definitive evidence on the presence of the Madhupur blind fault, it is considered to be an important active fault for the seismic hazard assessment of Dhaka, the capital of Bangladesh, since the fault extends towards Dhaka.

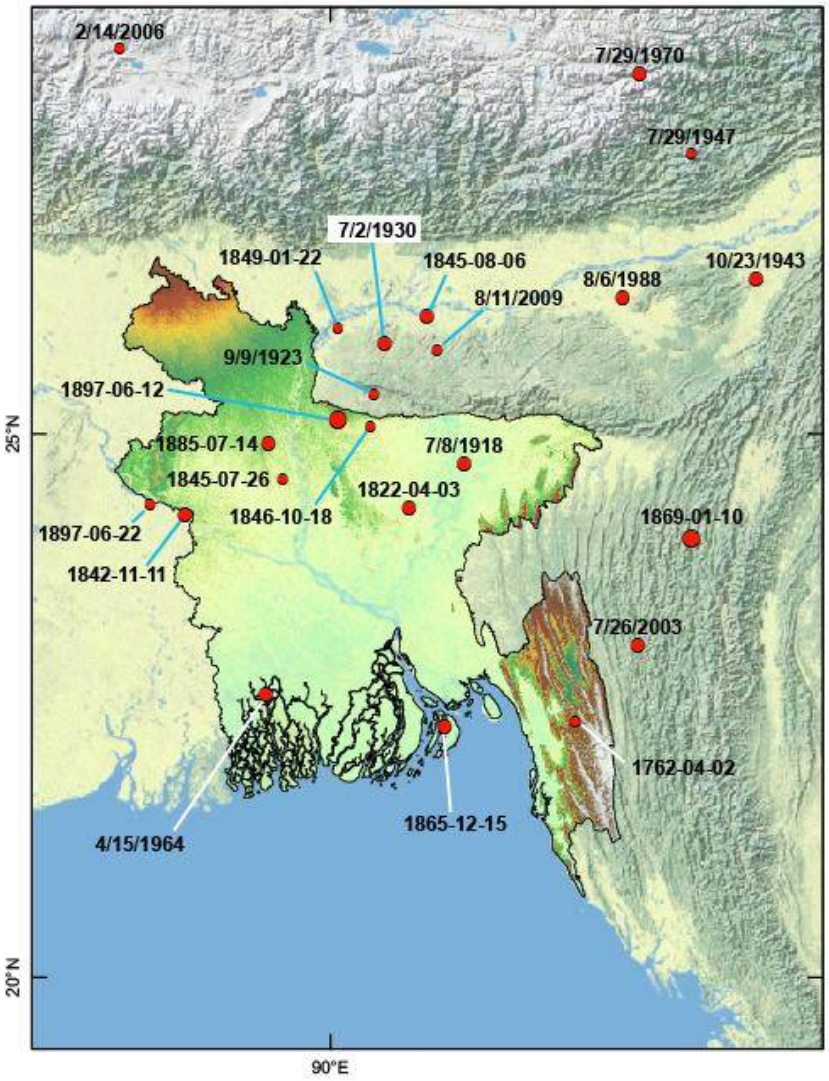

Figure 4. Large (M>6) historical earthquakes in the catalogue of Szeliga et al. (2010). Extracted from the figure of EOS draft report.

Table 1　Major historical earthquakes in and around Bangladesh. The 1885 Bengal earthquake is added in the table of EOS draft report.

No.	Name	Date	M	Source area	References
1	–	1548	–	Dauki fault or Tripura segment	Iyengar et al. (1999) Steckler et al. (2008) Morino et al. (2011)
2	–	1676	–	CTFB or Tripura segment	Iyengar et al. (1999) Martin and Szeliga (2010)
3	Arakan earthquake	1762	8.5	Arakan segment	Halstead (1841) Oldham (1883) Martin and Szeliga (2010)
4	Bengal earthquake	1822	7.1	CTFB?	Martin and Szeliga (2010)
5	–	1842	7.3	Western Bengal	Ambraseys and Dauglas (2004) Martin and Szeliga (2010)
6	–	1845	7.1	Shillong Plateau?	Martin and Szeliga (2010)
7	–	1865	6.8	Arakan segment?	Martin and Szeliga (2010)
8	Cachan earthquake	1869	7.4 8.3	Indo-Burman ranges or Tripura segment	Ambraseys and Dauglas (2004) Martin and Szeliga (2010)
9	Bengal earthquake	1885	7.1	Madhupur blind fault?	Martin and Szeliga (2010) Middlemiss (1885)
10	Great Assam earthquake	1897	8.0	Dauki fault	Oldham (1899) Richter (1958) Abe (1994) Martin and Szeliga (2010)
11	Srimongal earthquake	1918	7.4	CTFB or Tripura segment	Stuart (1920 Martin and Szeliga (2010)

2.3 GPS data

Dr. S. H. Akhter offered unpublished GPS data in Bangladesh and its interpretation to us (Figs. 5a to 5e).

The shortening across the Tripura segment is sharply changed between longitude 91°and 92° (Fig. 5c), while the deformation may reach the buried thrust front. Dr. S. H. Akhter estimated the shortening strain across the buried thrust front and the Tripura segment on the western margin of the CTFB to be 2 mm/year and 5 mm/year, respectively (Fig. 5d).

Steckler et al. (2008) suggested that the mega-thrust front is located on the western edge of the Comilla Tract (buried thrust front in Fig. 5c). However, the velocity of GPS stations across the buried thrust front is too small with 2 mm/year. We consider that the Tripura segment is located on the western margin of the CTFB.

The GPS stations of CHNR, MKCH, and SITA tend to subside, while the GPS stations of BAGH and KPTI, which are located more east, are not subsiding. The western margin of the Burman plate must be usually subsiding and be abruptly uplifted during large earthquakes.

The accumulation of shortening strain across the Dauki fault is estimated to be 7 mm/year (Fig. 5e).

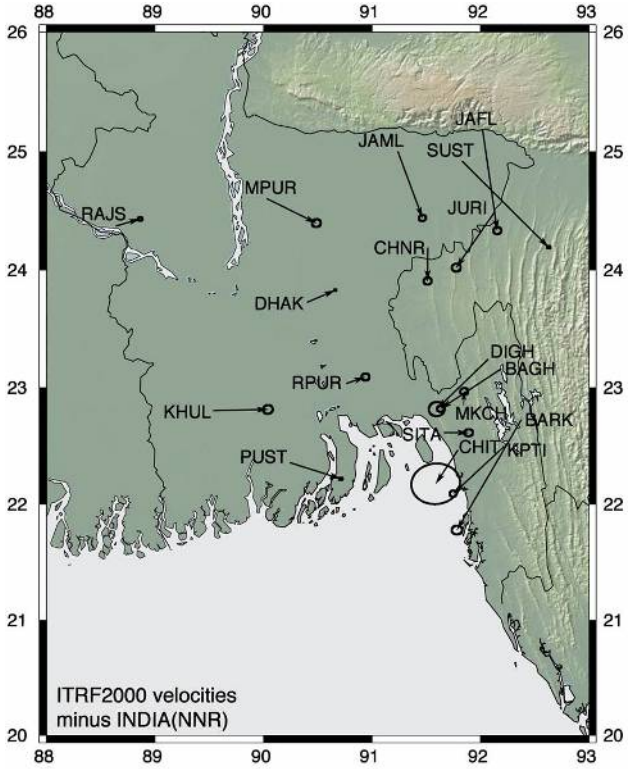

Figure 5a. Motion of GPS stations relative to the Indian plate. Courtesy of Dr. S. H. Akhter.

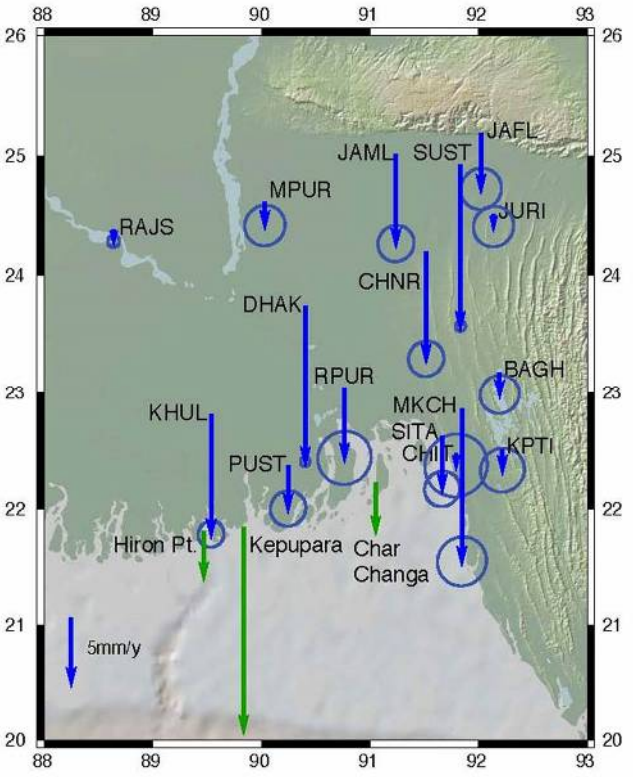

Figure 5b. Vertical motion of GPS stations. Courtesy of Dr. S. H. Akhter.

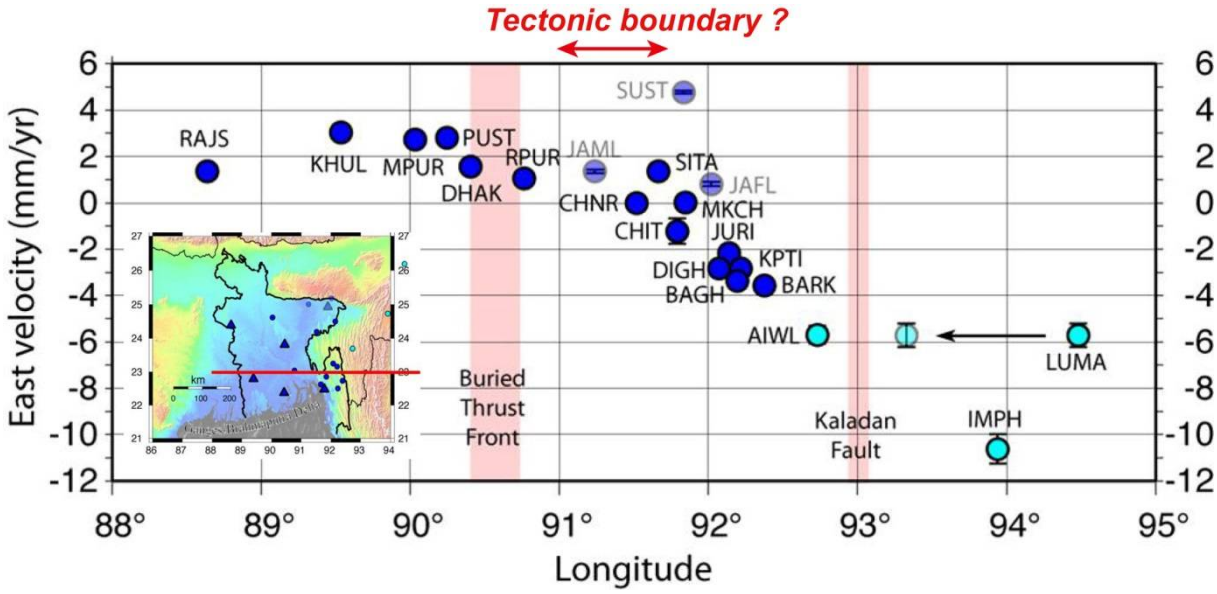

Figure 5c. Accumulation of shortening strain across the Tripura segment. Courtesy of Dr. S. H. Akhter. The tectonic boundary is added by us.

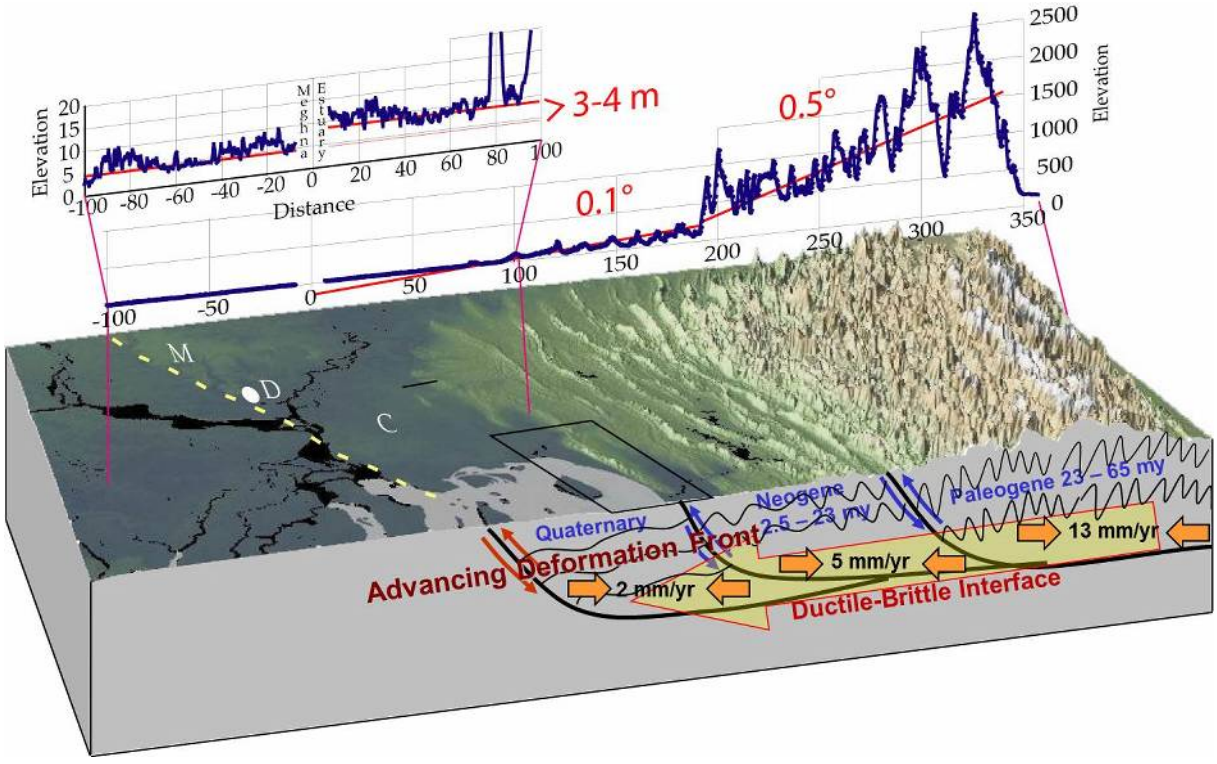

Figure 5d. Slip rate across the buried thrust front and the Tripura segment interpreted by S. H. Akhter.

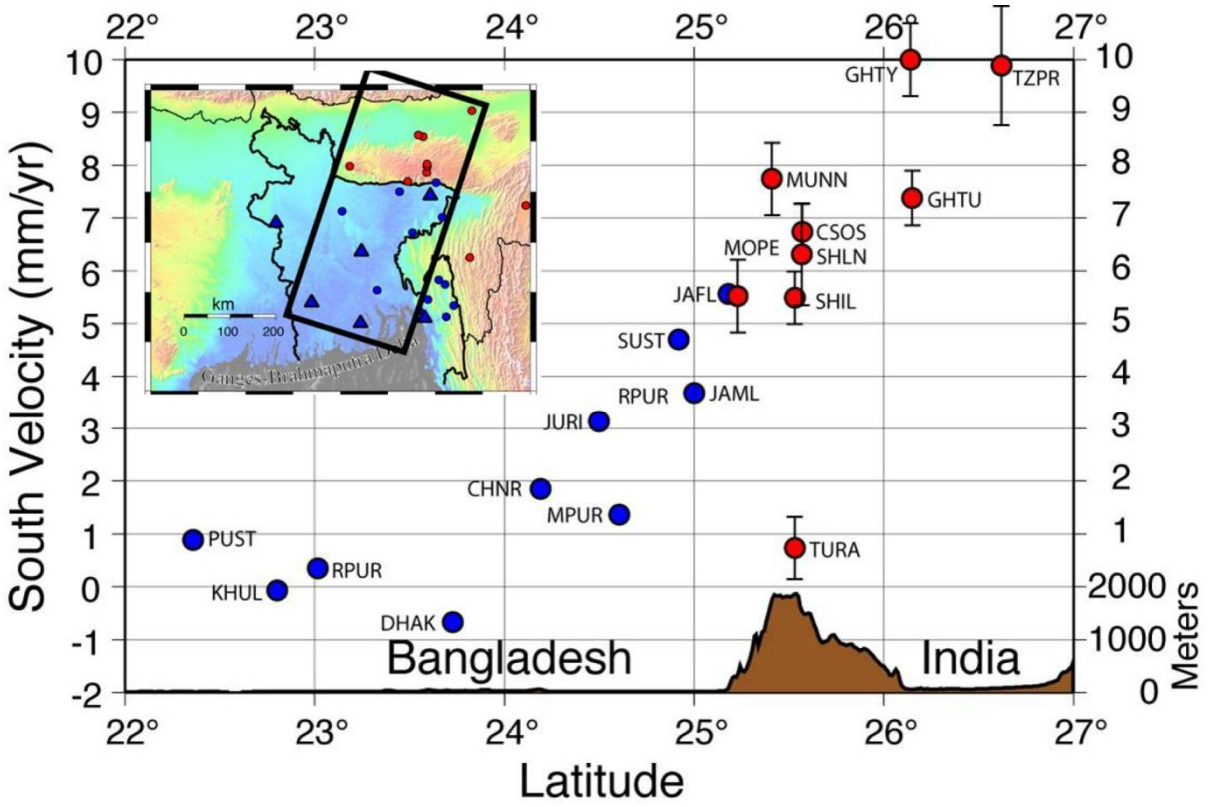

Figure 5e. Accumulation of shortening strain across the Dauki fault. Courtesy of Dr. S.H. Akhter.

3. Tectonic geomorphic investigation

The satellite photo interpretation of CORONA and ALOS was carried out, and the tectonic geomorphology was confirmed in the field. The tectonic geomorphology in Bangladesh is not clear. The fault or warping scarp tends to be eroded and buried by rapid sedimentation due to abundant rainfall. Furthermore, Bangladesh is a densely populated country, so the geomorphology is modified by the severe agriculture and road construction.

3.1 Dauki fault

The hills, which are composed of Tertiary and Quaternary sediments, are developed at the southern foot of the Shillong Plateau, and narrow terraces are identified at the southern foot of the hills. It is thought that the hills and terraces are uplifted by the activity of the Dauki fault, and active faults are inferred at the southern edge of the terraces. This is indicative of the foreland migration of the Dauki fault. The uplifted terraces are identified by the satellite photo interpretation. However, it is difficult to detect the deformation of terrace surface due to low resolution of the satellite photo. We confirmed the deformation of the terrace surface in the field. Back-tilted lower terraces were identified at Gabrakhari and Jaflong.

The CORONA satellite photo around Gabrakhari is shown in Fig. 6. Narrow terraces are developed at the southern foot of the hill, and an active fault is inferred at the southern edge of the terrace. The fault scarp is clear in the left top of Fig. 6. However, this area stands on India. We investigated the eastern area which is in Bangladesh, and the back-tilted terrace was identified at Gabrakhari (Figs. 7 to 9). The terrace, which is covered by gravel layer, shows a pressure ridge and the northern wing is back-tilted. This demonstrates a typical tectonic geomorphology, and an active fault is inferred at the southern edge of the terrace.

The geomorphology around Jaflong is composed of the Shillong Plateau, hills, terraces, and Alluvial lowland from the north to the south (Fig. 10). Two active faults are inferred around Jaflong. The straight steep scarp is recognized on the southern margin of the Shillong Plateau. The topographic drop across the scarp is clear. An active fault is inferred on the southern margin of the Shillong Plateau. The lower terrace is developed at the southern foot of the hills (Figs. 11 and 12). An active fault is inferred on the southern edge of the terrace, since the terrace is uplifted. According to Bangladesh geological map, the northern fault is estimated to be the Dauki fault, and the southern fault represents a foreland migration of the Dauki fault. We tentatively call the southern one jaflong fault. The southern Jaflong fault

continues to the east stepping to the south, while the fault scarp of the northern fault becomes obscure eastwards. It is inferred that the Jaflong fault is more active than the Dauki fault around Jaflong.

The detailed field survey revealed that the lower terrace is back-tilted and the terrace is covered by gravel layer with fresh pebbles and cobbles (Figs. 13 and 14). It is thought that the lower terrace was created by the uplift of younger channel.

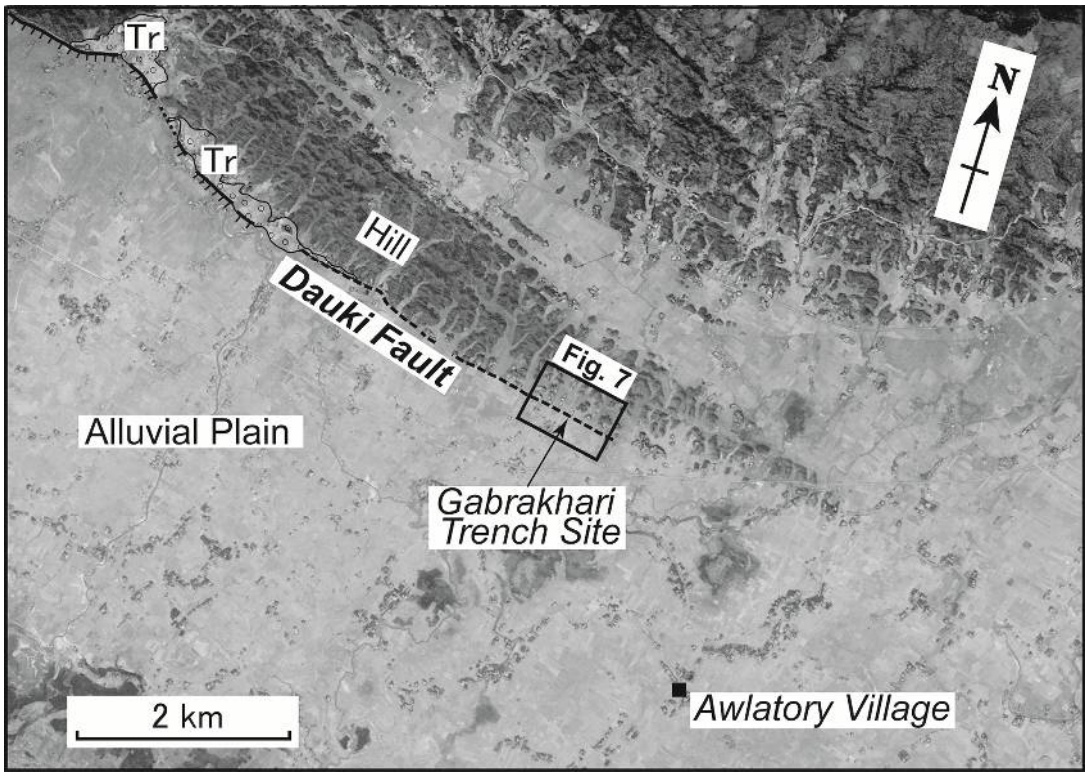

Figure 6. CORONA satellite photo around Gabrakhari

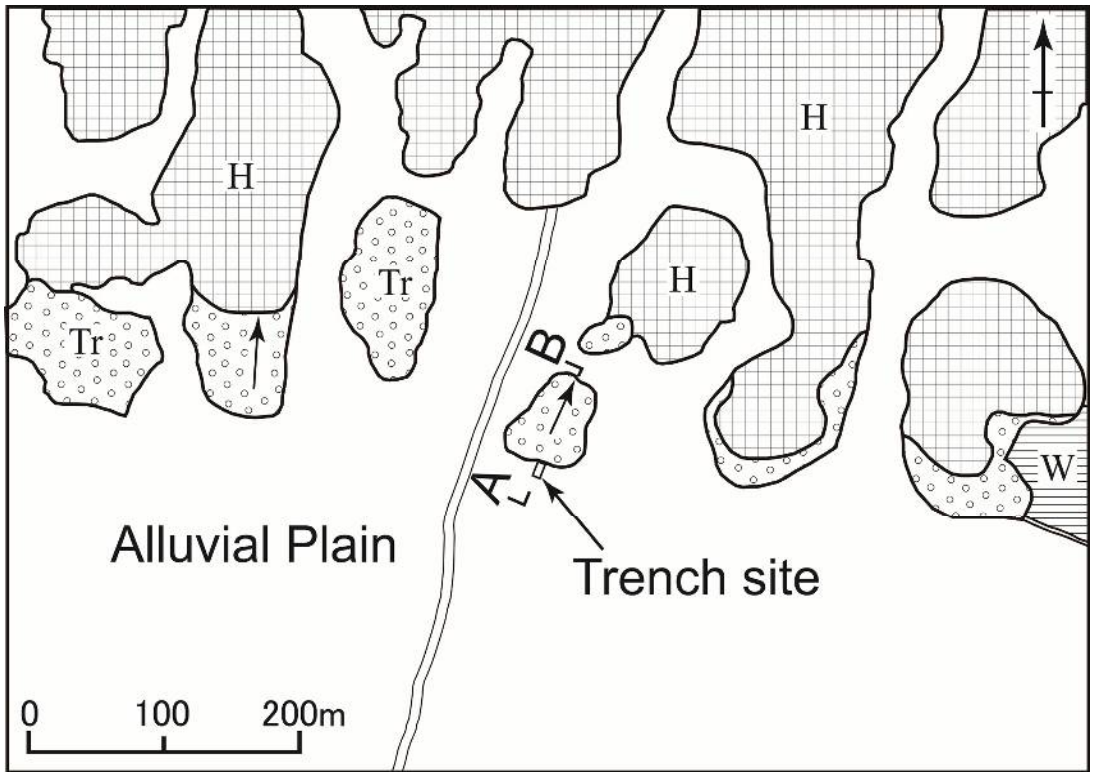

Figure 7. Geomorphic map around Gabrakhari. The location is shown in Fig. 6. H: hill, Tr:

lower terrace. Arrows represent back-tilted terraces.

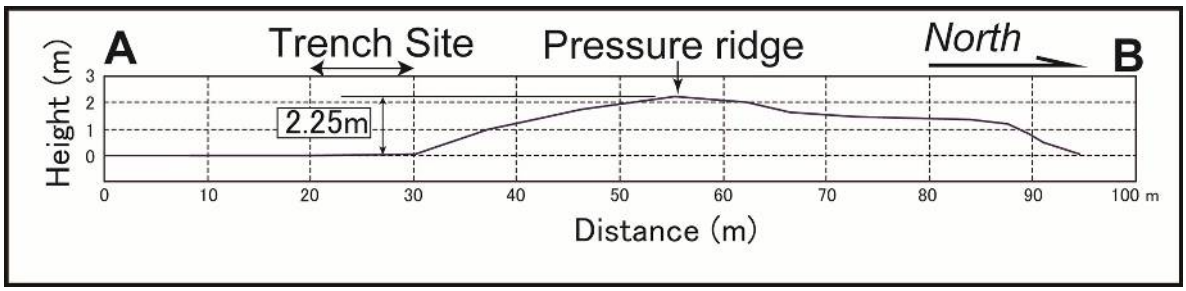

Figure 8. Topographic profile across the lower terrace. The location of the profile is shown in Fi. 7.

Figure 9. Photo showing the back-tilted terrace. View is towards the west.

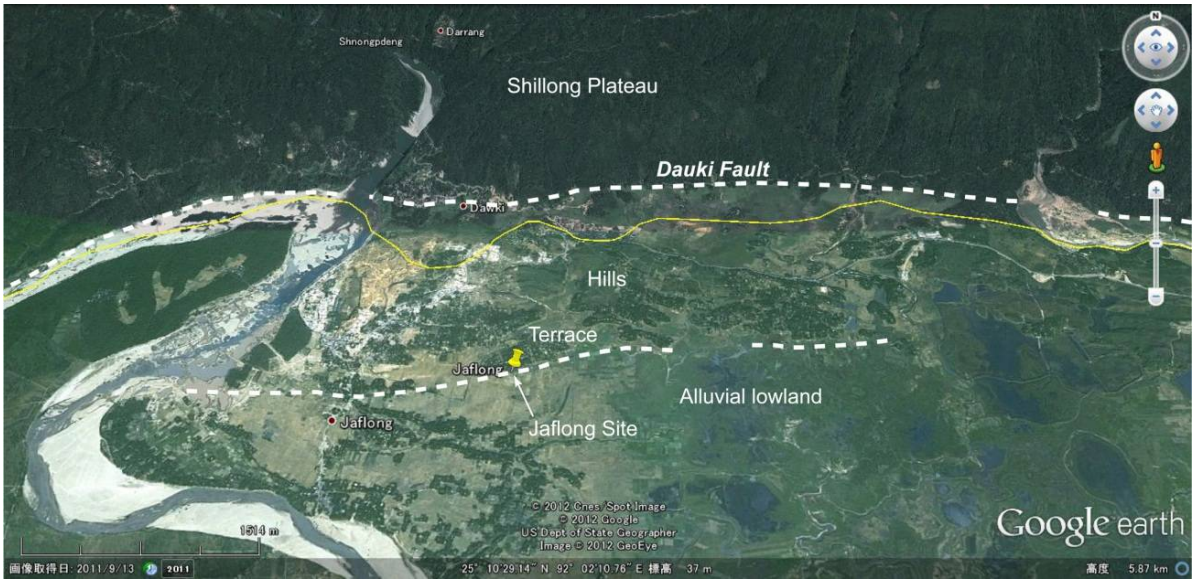

Figure 10. Geomorphology around Jaflong. White broken lines represent active faults.

Figure 11. Photo showing geomorphology around Jaflong. View is towards the north. The top, middle, and bottom steps are composed of the Shillong Plateau, hills, and lower terrace, respectively. Bamboo grows thickly on the lower terrace.

Figure 12. Close view of the lower terrace. The trench was excavated at the place where people stand.

Figure 13. Gravel layer covering the terrace with fresh pebbles and cobbles.

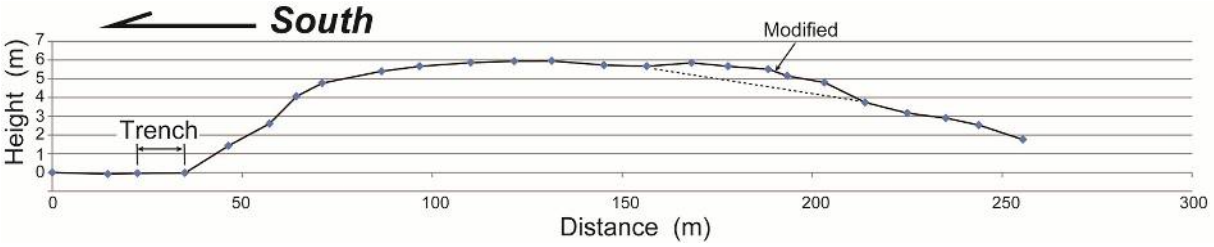

Figure 14. Topographic profile across the lower terrace. The terrace surface is back-tilted towards the north.

3.2 Indian-Burman plate boundary fault

The Indian-Burman plate boundary fault is inferred on the western margin of the Chittagong-Tripura Fold belt (CTFB). The satellite photo interpretation and field survey were carried out along the western margin of the CTFB, and tectonic geomorphologies were identified at Shahzibazar, Kasba, Comilla Hill, and Maheshkhali (Fig. 1).

1) Shahzibazar, Habiganj

According to the seismic reflection survey across the Habiganj gas field, the anticline is developed in the gas field, and an east-dipping active blind fault is identified on the west limb (Fig. 15). The Dupi Tila formation in the Late Quaternary time overlies the Tipam formation in Early Quaternary time with angular unconformity. The Dupi Tila formation thins towards the crest of the anticline. This means that the Dupi Tila formation was deposited together with fold growth (Johnson and Nur Alam, 1991).

The CORONA satellite photo around Shahzibazar, Habiganj is shown in Fig. 16. The Habiganj gas field is located on the hill, and the warping scarp was identified at 2-3 km west from the hill. The eastern area of the scarp is considered to be a wide uplifted terrace which was made up by the activity of an active blind fault.

2) Kasba

The back-tilted lower terrace was identified at Kasba (Fig. 17). The topographic profile is shown in Fig. 18. The lower terrace with height of ~4 m is back-tilted towards the east and merges into the Alluvial Plain (Fig. 19). The steep scarp is recognized on the western edge of the terrace. The back-tilted terrace is estimated to be tectonic geomorphology on the western margin of the CTFB. An active fault was inferred and the trench was excavated on the western edge of the terrace. However, we could not identify any fault and deformation in the trench. It is thought that the fault scarp is eroded and shifted to the east.

3) Comilla Hill

The Comilla Hill, which is located 12 km west from the CTFB (Fig. 1), is an isolated and a long mount with N-S direction (Fig. 20a). The surface is gently inclined to the east (Figs. 20b and 20c). The surface is back-tilted as well as Kasba. The steep scarp at the western edge of the hill is inferred to be a fault scarp. However, no active fault was identified in the trench. The scarp may be eroded.

4) Maheshkhali

Most of the Arakan segment passes in the sea and there are few places where are able to observe the tectonic geomorphology. Only at Maheshkhali, a low scarp with N-S direction is identified (Fig. 21). In the south of Maheshkhali, the eastern side of the low scarp seems to be uplifted. The low scarp is straight, so it is thought to be a fault scarp. However, it may be an eroded scarp of the uplifted marine terrace. We visited Maheshkhali to confirm a low scarp. But, the low scarp was filled by the water, since the dam was built on the western footwall of the scarp.

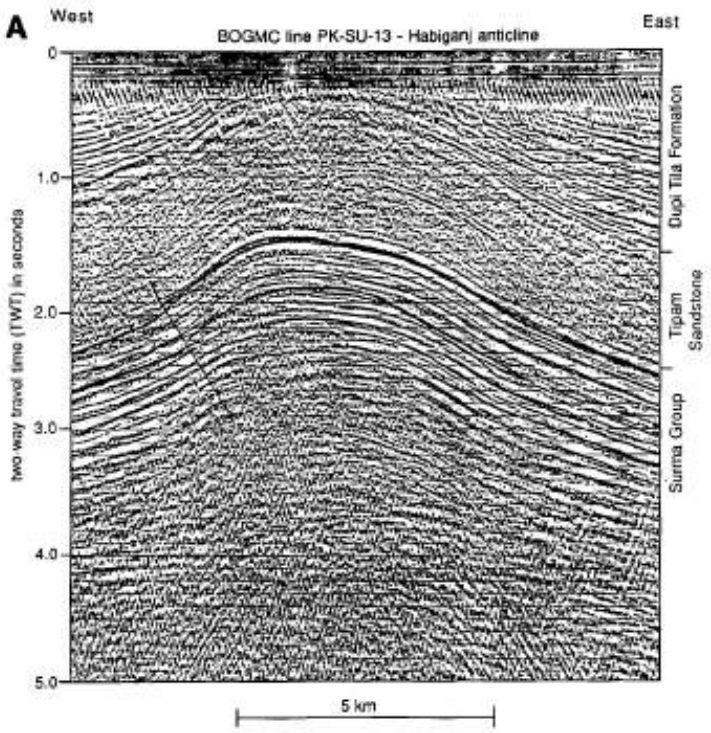

Figure 15. The seismic reflection section across the Habiganj gas field (Johnson and Nur Alam, 1991). A reverse fault is inferred on west limb.

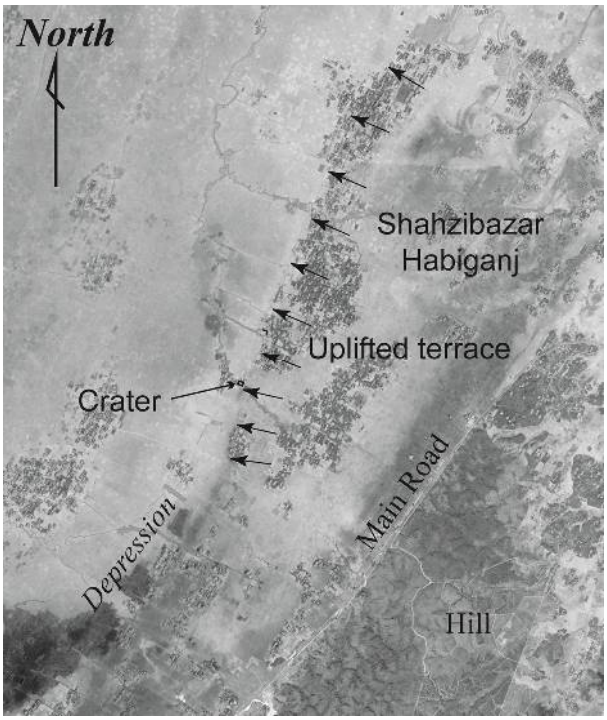

Figure 16. The warping scarp identified at Shahzibazar, Habiganj. The background is CORONA satellite photo. Arrows represent warping scarp. The eastern area of the scarp is uplifted with 2-3 km wide. The Habiganj gas field is located at right top.

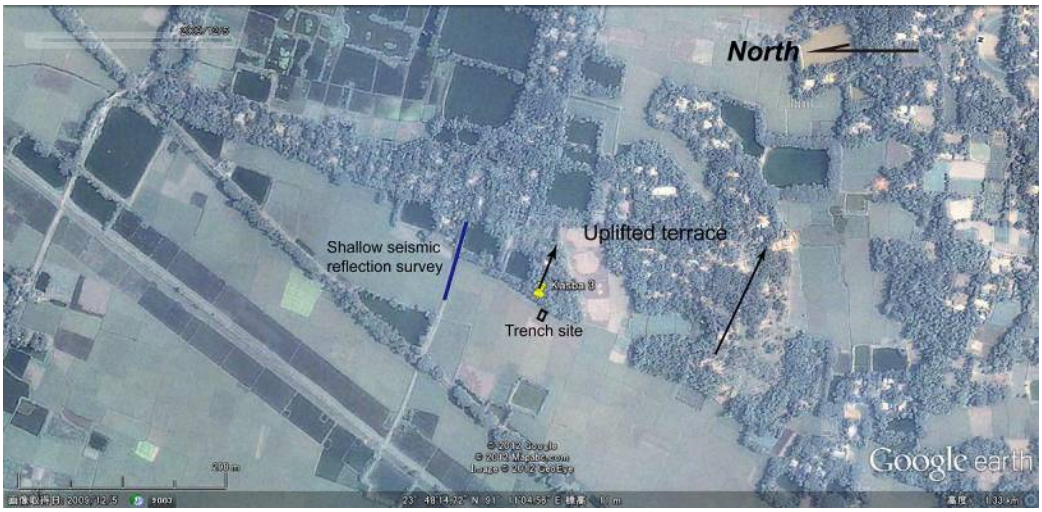

Figure 17. Back-tilted terrace at Kasba. The arrows represent back-tilted surface. A shallow seismic reflection survey is planned.

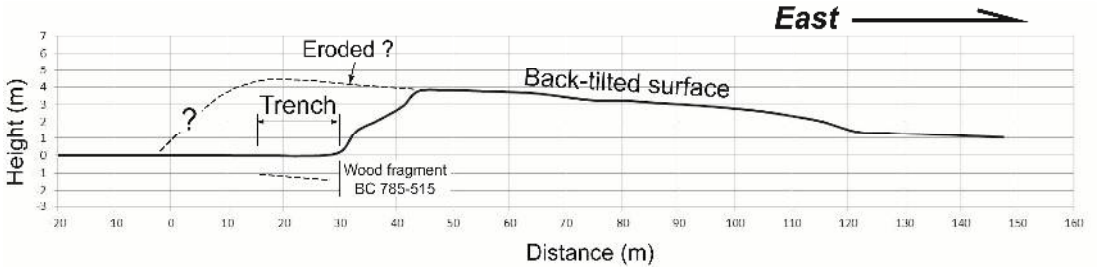

Figure 18. Topographic profile across the trench site. The layers in the trench is gently inclined to the east. The fault scarp is eroded. The wood fragment collected in the trench is dated to 785-515 BC.

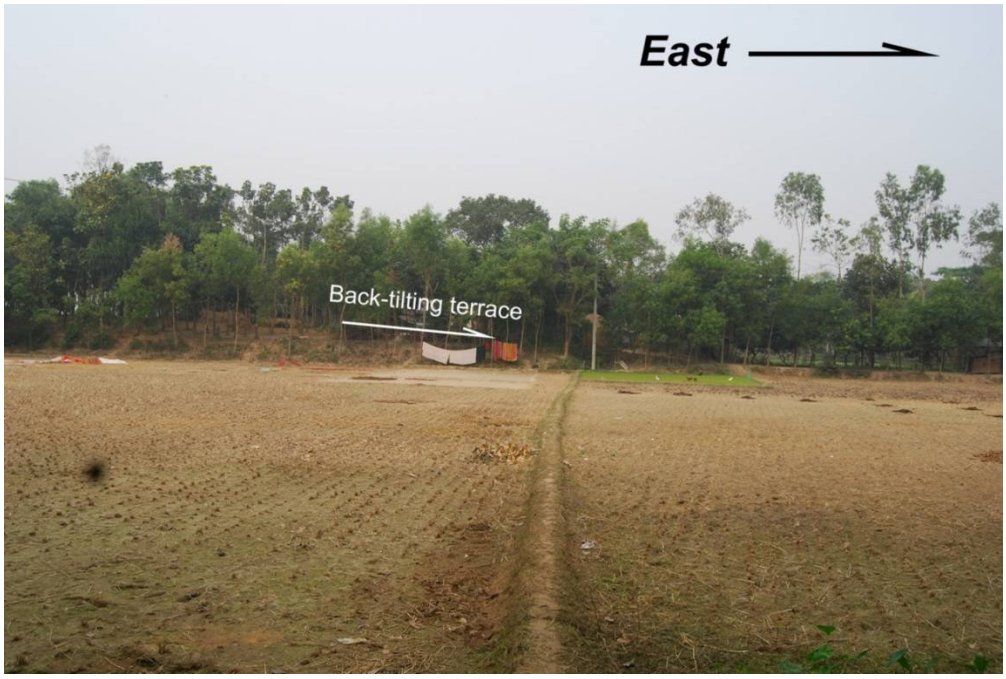

Figure 19. Photo showing a back-tilted terrace. View is towards the north.

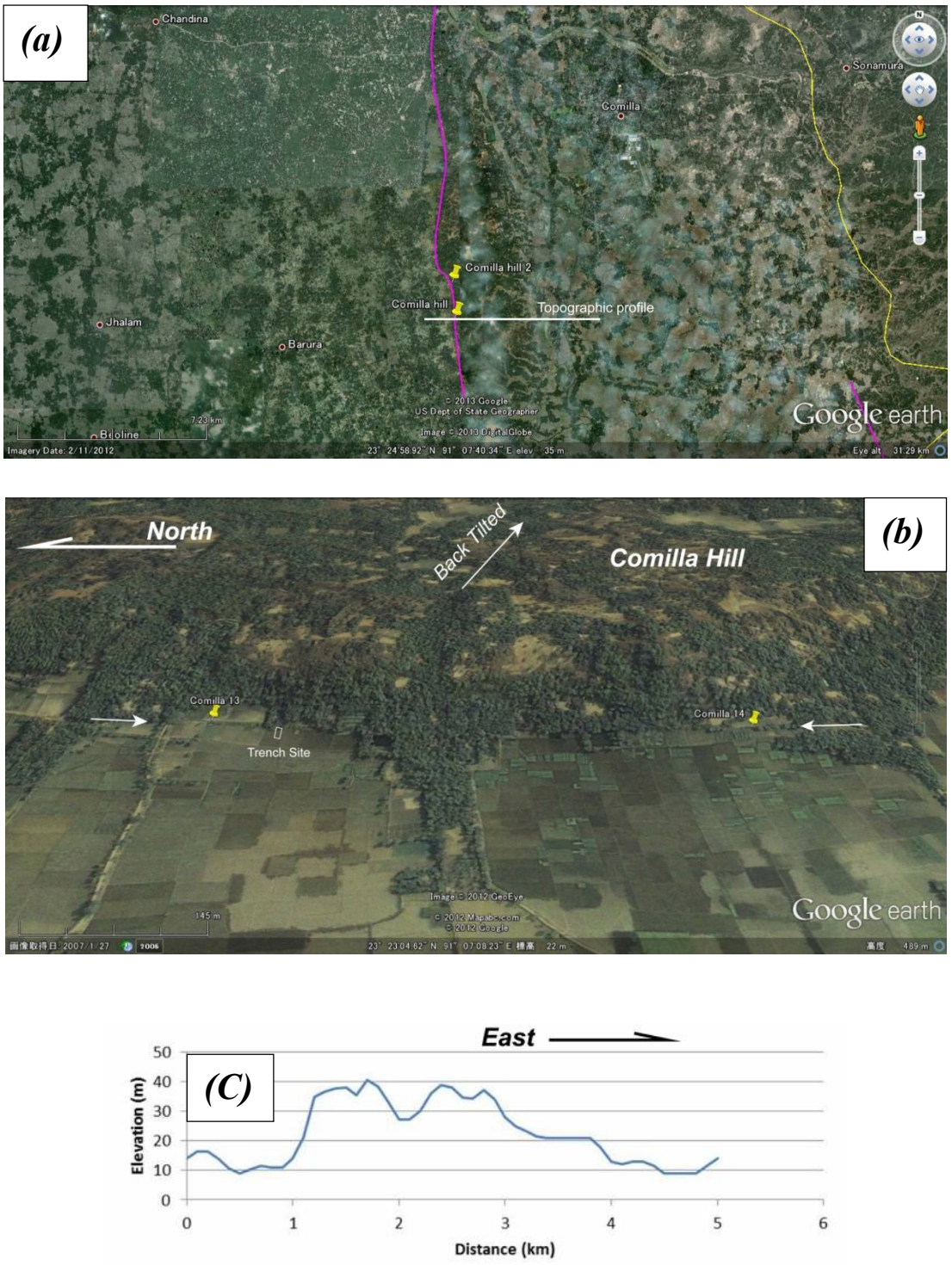

Figure 20. (a): Location of the Comilla Hill, which is long with N-S direction. (b): Geomorphology of the Comilla Hill. The surface is gently back-tilted towards the east. The steep scarp is recognized at the western edge of the hill. The trench was excavated at the foot of the scarp. (c): Topographic profile across the Comilla Hill. The profile was made from SRTM data.

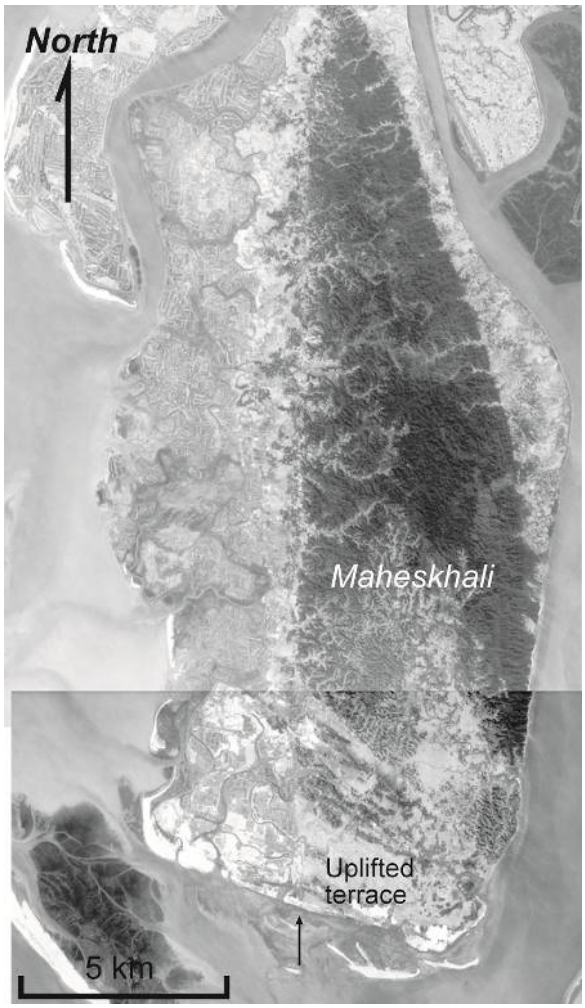

Figure 21. A low scarp at Maheshkhali. The eastern side is uplifted. The low scarp is thought to be a fault scarp, since it is straight. However, it may be an eroded scarp of the uplifted marine terrace. The dam is built on the west of the scarp and the scarp is filled by water at present.

3.3 Active faults within Chittagong-Tripura Fold Belt

A number of anticlines are developed within the Chittagong-Tripura Fold Belt (CTFB). If a younger surface such as Alluvial surface is deformed at the foot of anticlinal hill, it is an active structure. However, these structures may be secondary and inactive at present, since these structures might be made up in the process of the westward migration of the Tripura segment.

1) Hararganj anticline

According to high-resolution satellite photo interpretation, the northernmost part of the Hararganj anticline may deform a young fluvial surface (EOS draft report). The anticline is active and a blind active fault is inferred.

2) Fenchunganj anticline

According to high-resolution satellite photo interpretation, a low scarp is recognized at the eastern foot of the hill where the Fenchunganj anticline is manifest. The low scarp is inferred to be a fault scarp or warping scarp, since it is identified on the young fluvial surface (EOS draft report).

3) Sylhet anticline

The ENE-WSW long hill is developed on the north of Sylhet (Fig. 22a). The seismic reflection profile at the northeastern edge reveals that an anticline with ENE-WSW axis is identified in the hill, and the Dupi Tila formation in the Late Quaternary time shows the sedimentary process of growth strata that the layers thin towards the crest of the fold (Johnson and Nur Alam, 1991; Steckler et al., 2008). The topographic profile across the hill represents a symmetrical folding of the surface (Fig. 22b). This indicates that the Dupi Tila formation was deposited together with the growth of the active anticline. The Sylhet anticline is active and an active blind fault is inferred beneath the hill.

4) Rashidpur anticline

The Dupi Tila formation of the Bibiyana anticline, which is the northern extension of Rashidpur anticline, shows growth strata. Both anticlines are active and an active fault is inferred. We infer an active fault at the western foot of the anticlinal hill, while EOS draft report suggests an active fault at the eastern foot of the anticlinal hill. A fault scarp is obscure,

since the highway to Sylhet is constructed along the western foot of the hill. On the exposure along the highway, the Dupu Tila formation is steeply inclined to the west.

5) Jaldi anticline

The seismic reflection profile indicates that active faults are inferred on both limbs of the Jaldi anticline (Maurin and Rangin, 2009). EOS draft report suggests that a fault scarp is inferred on the young fluvial surface at the western foot of the anticlinal hill.

6) Dakshin Nila anticline

The Dakshin Nila anticline shows asymmetric topographic profile with the western steep slope and the eastern gentle slope, and a fault scarp is inferred at the western foot of the hill (EOS draft report). According to our preliminary field survey from Cox' Bazar to Teknaf, several steps of uplifted marine terraces are developed along the western foot of the hill. The straight low scarp is thought to be an eroded one.

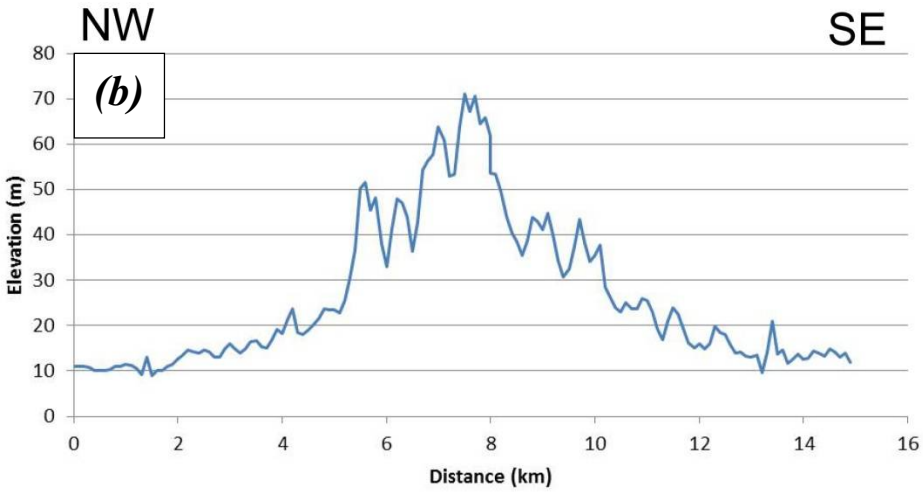

Figure 22. (a): Location of Sylhet anticline. (b): Topographic profile across the Sylhet anticline.

3.3 Madhupur blind fault

Although the Madhupur Tract is heavily eroded, the crests of the hill keep flat surfaces which are gently tilted to the east (Figs. 23a and 23b). The straight low scarps are developed at the western edge of the Tract. The low scarps are estimated to be fault scarps, and the east-dipping Madhupur blind fault is inferred from these geomorphic features. The Madhupur blind fault is considered to be important for seismic hazard assessment of Bangladesh, since Dhaka, the capital of Bangladesh, stands ~40 km southeast from the fault. However, no deformation is identified on the young fluvial surface, so the low scarps may be eroded ones. The Madhupur Tract is uplifted by the activity of the Madhupur blind fault. However, the warping scarp is thought to be eroded.

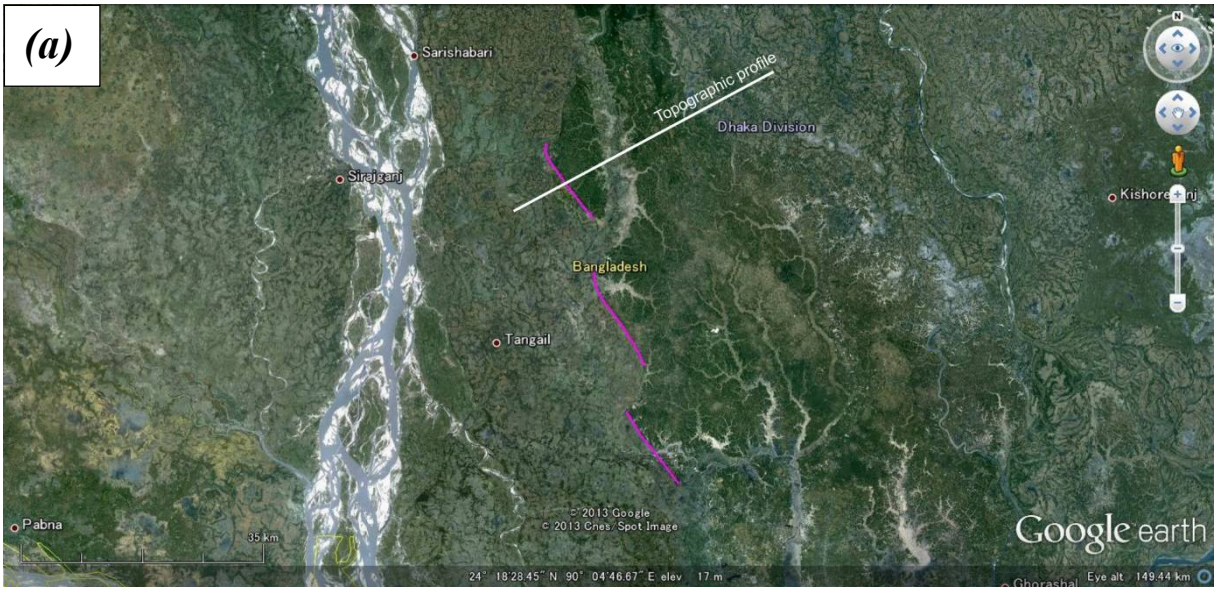

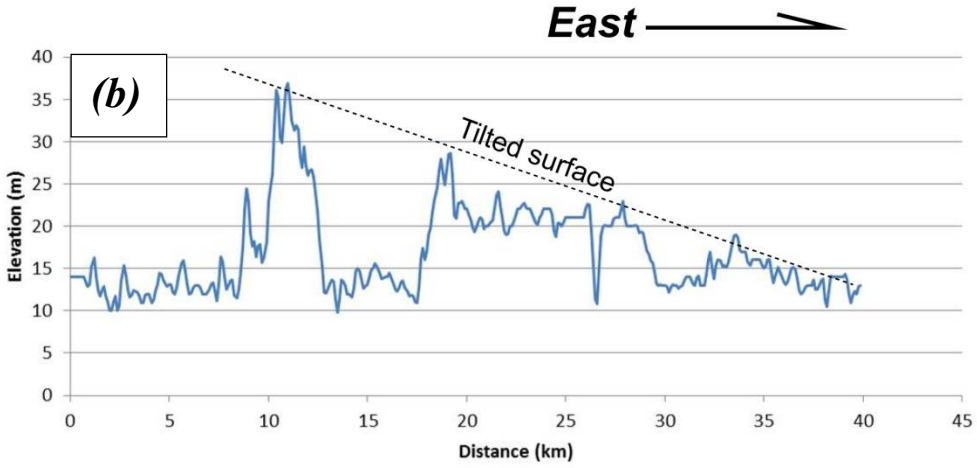

Figure 23. (a): Madhupur blind fault inferred on the western margin of the Madhupur Tract. (b): Topographic profile across the Madhupur Tract. The hill is heavily eroded. However, the crests keep a flat surface and tilted to the east.

4. Trench investigation

We carried out the trench investigation across the Dauki fault and the Tripura segment in order to reveal the timing of the seismic events.

4.1 Dauki fault

The trench investigation across the Dauki fault was carried out at two sites of Gabrakhari and Jaflong (Fig. 1). The result of the trench investigation at Gabrakhari is published by Morino et al. (2011). The result will be shortly mentioned.

1) Gabrakhari site

The log of the west wall at Gabrakhari trench site is shown in Fig. 24. The small fault strands, F1, F2, and F3, were identified in the trench. These faults displace units G and H, and are covered by unit F with unconformity. The seismic event has occurred between the deposition of units F and G. The sand dikes due to paleo-liquefaction were identified in the trench. The sand dikes reach to the top of unit B and are covered by unit A. At Awlatory (Fig. 6), a lot of sand dikes were identified on the wall of the pond which was dug in the Alluvial Plain (Fig. 26). The sand dikes are inferred to be created at the same time with Gabrakhari site, since the sand dikes reach close to the surface.

The timing of the seismic event that is inferred from F1 to F3 faults is dated to AD 1500-1630. This corresponds to the 1548 earthquake (Fig. 25). The paleo-liquefaction is created after AD 1700. This corresponds to the 1897 Great Assam earthquake, while there is no evidence that the Dauki fault has ruptured in 1897 around Gabrakhari.

The displacement of F1 to F3 fault is small as large as several 10 cm. However, the terrace surface is deformed with 60-70 m wide. If the deformation on the hanging wall is considered, the displacement must be larger.

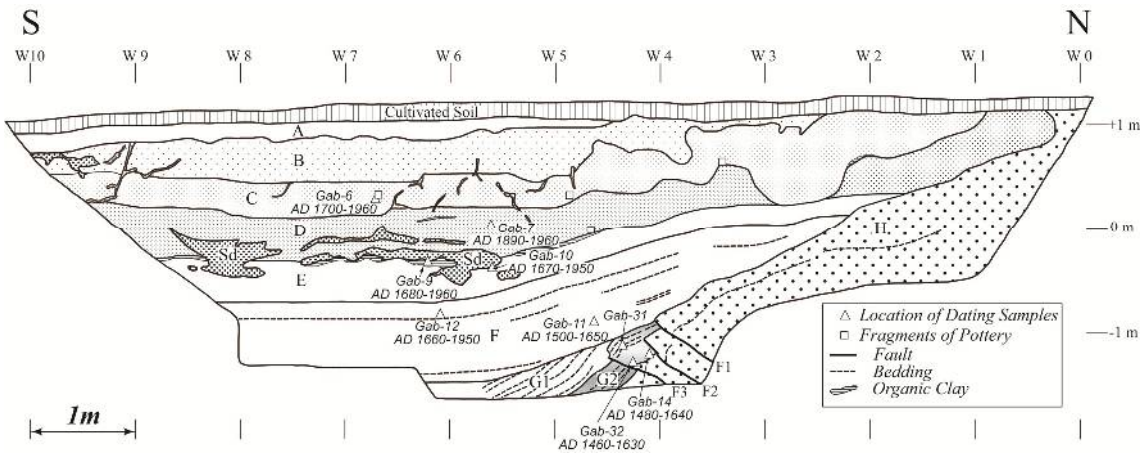

Figure 24. Log of the west wall at Gabrakhari trench site. The stratigraphy in the trench is divided into units A to H. Small fault strands, F1, F2, and F3 are identified. Sd: Sand dikes due to paleo-liquefaction.

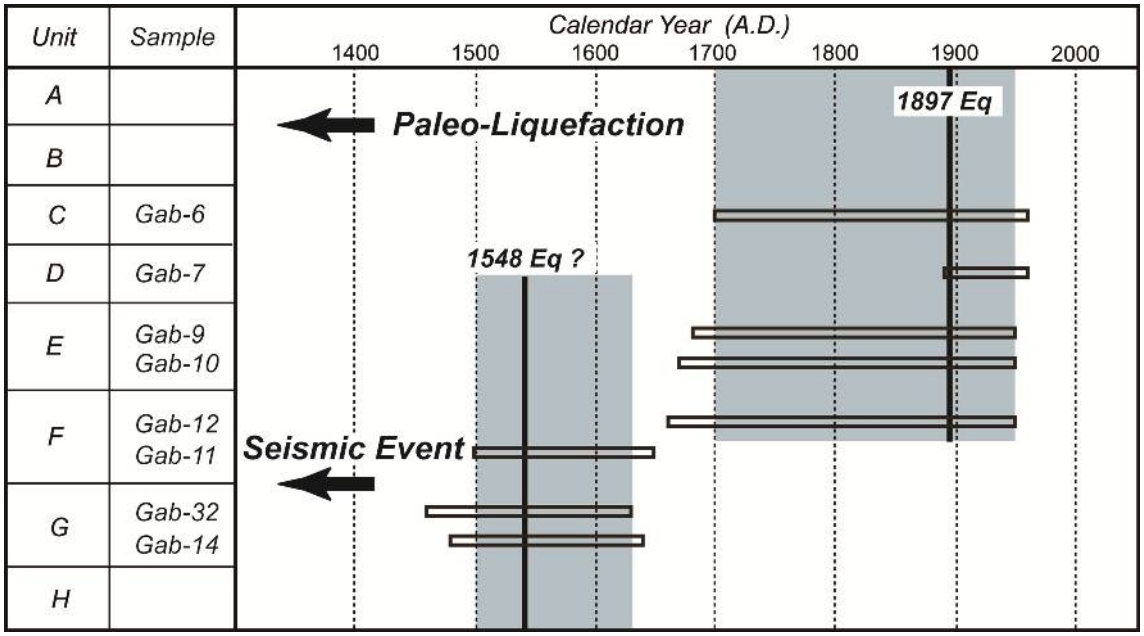

Figure 25. Timing of the seismic events inferred from the trench investigation at Gabrakhari site.

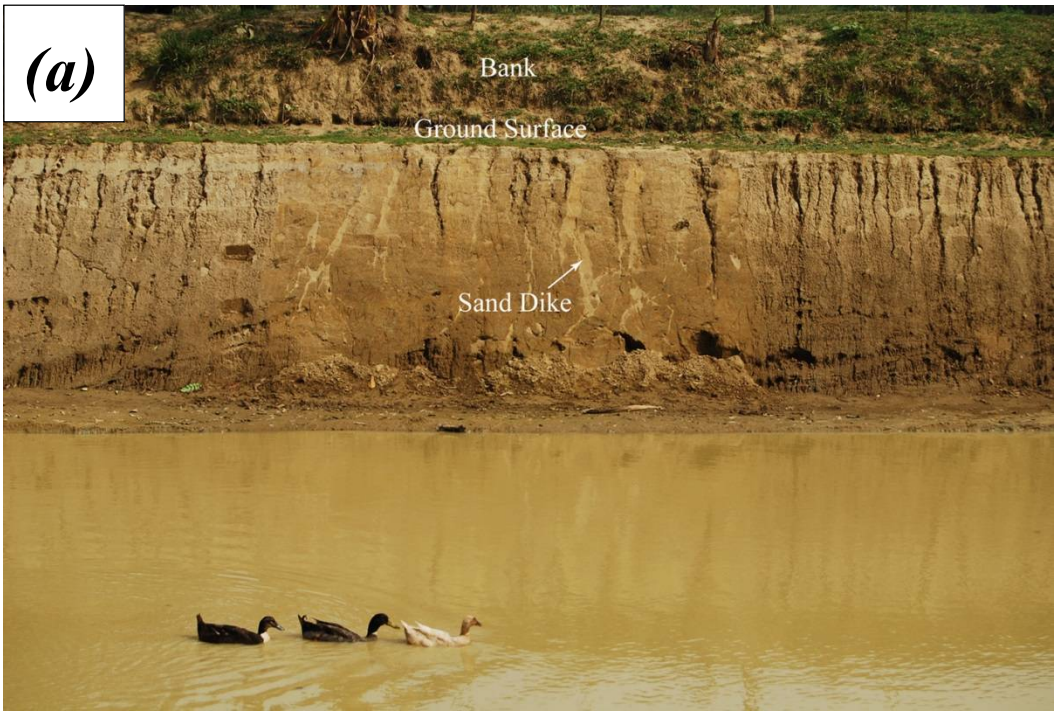

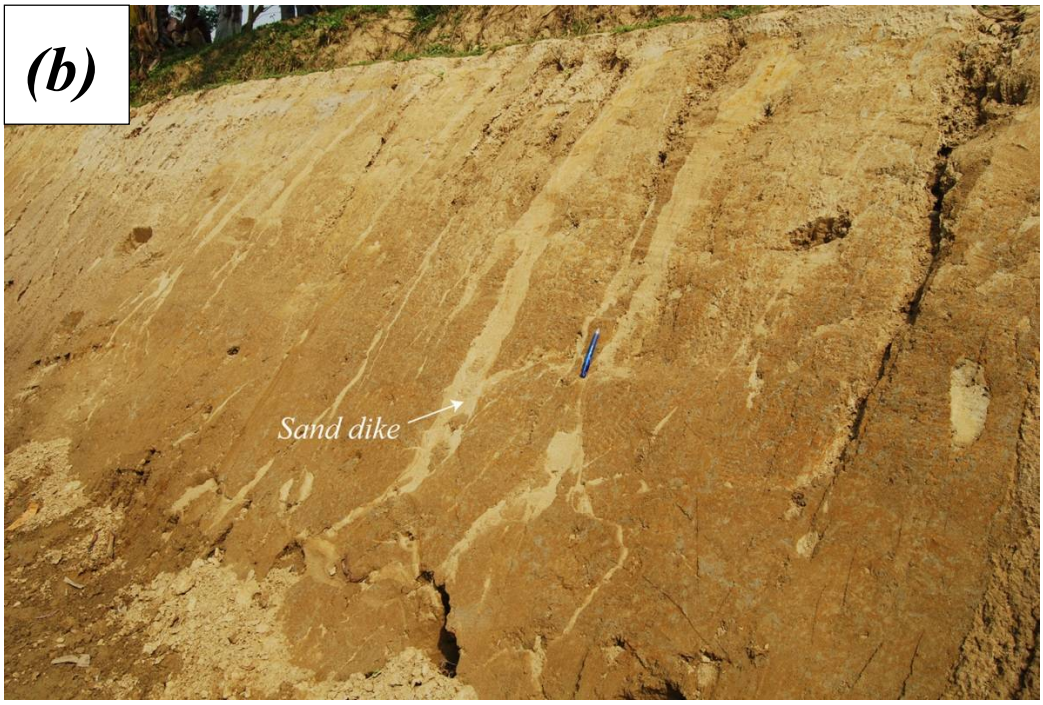

Figure 26. (a): Sand dikes due to paleo-liquefaction at Awlatory. The pond is dug in the Alluvial Plain, and sand dikes were identified on the walls. (b): Close view of sand dikes.

2) Jaflong site

The back-tilted lower terrace was identified at Jaflong, the north of Sylhet. The trench investigation at two sites of Jaflong 1 and Jaflong 2 was carried out (Morino and Kamal, 2012).

Stratigraphy identified in the trench and its radiocarbon age

The log and mosaic photo of west wall at Jaflong 1 site are shown in Figs. 27 and 28, respectively. The result of ^{14}Cdating is shown in Table 2. The stratigraphy in the trench is divided into the upper unit and the lower unit. The upper unit is divided into subunits A to C, and the lower is divided into subunits Ⅰ to Ⅳ.

Unit A: Blackish organic silt. The radiocarbon age of organic silt shows AD 1270-1390 (Jaf-5).

Unit B: Yellowish brown medium sand.

Unit C: Stratified alternation of gray silt and fine sand. The radiocarbon age of organic silt with charcoals shows AD 900-1020 (Jaf-4).

Unit Ⅰ: Stratified alternation of whitish yellow brown silt and fine sand. This layer shows a similar face with unit C. However, the top of this layer shows white-color, and a warping structure is clear between horizontal markers W1 and W4. This layer is overlain by units A to C with unconformity (Figs. 29a to 29d).

Unit Ⅱ: Gray and yellowish brown silt. The organic silt with charcoals is dated to AD 730-940 (Jaf-2).

Unit Ⅲ: Gray and whitish gray silt. The charcoal (Jaf-3) and organic silt with charcoals (Jaf-1) are dated to AD 640-990.

Unit Ⅳ: Gravel with sub-rounded pebbles-cobbles of 0.5-2 cm in average diameter and ~10 cm in maximum diameter. The matrix is composed of brown sandy silt.

Flexure structure

Units Ⅰ to Ⅳ show a flexural structure and are covered by units A to C unconformably. The seismic event, which made up the unconformity, is inferred between units C and Ⅰ. As shown in Figs. 29a to 29d, the flexural structure is clear.

Another trench investigation at Jaflong 2 was performed at the eastern side close to Jaflong 1 site in order to excavate a deeper trench. However, the water has sprung from gravel layer of unit Ⅳ and sometimes the trench was caught in showers, so the deeper trench could not be excavated. The trench at Jaflong 2 site resulted in the same depth as Jaflong 1. We

collected the dating samples from the trench at Jaflong 2 and considered the timing of the seismic event from these data. The log of the east wall at Jaflong 2 site is shown in Fig. 30.

Timing of the seismic event

The timing of the seismic event is dated to be AD 720-1020 from the result of ^{14}C dating. If the samples with young age are adopted, the timing is limited to AD 880-1020 (Fig. 31).

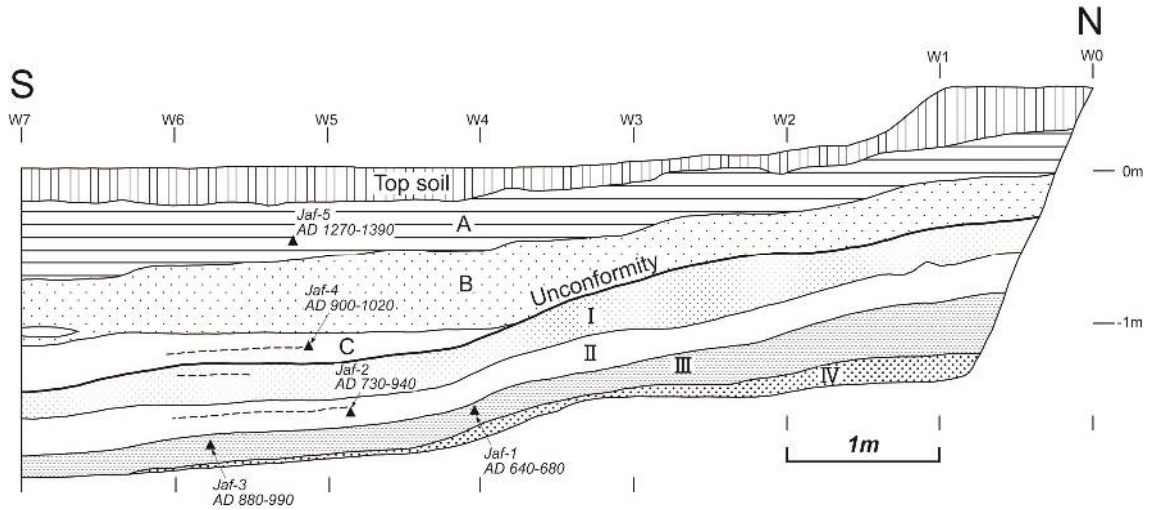

Figure 27. Log of the west wall at Jaflong 1 trench site

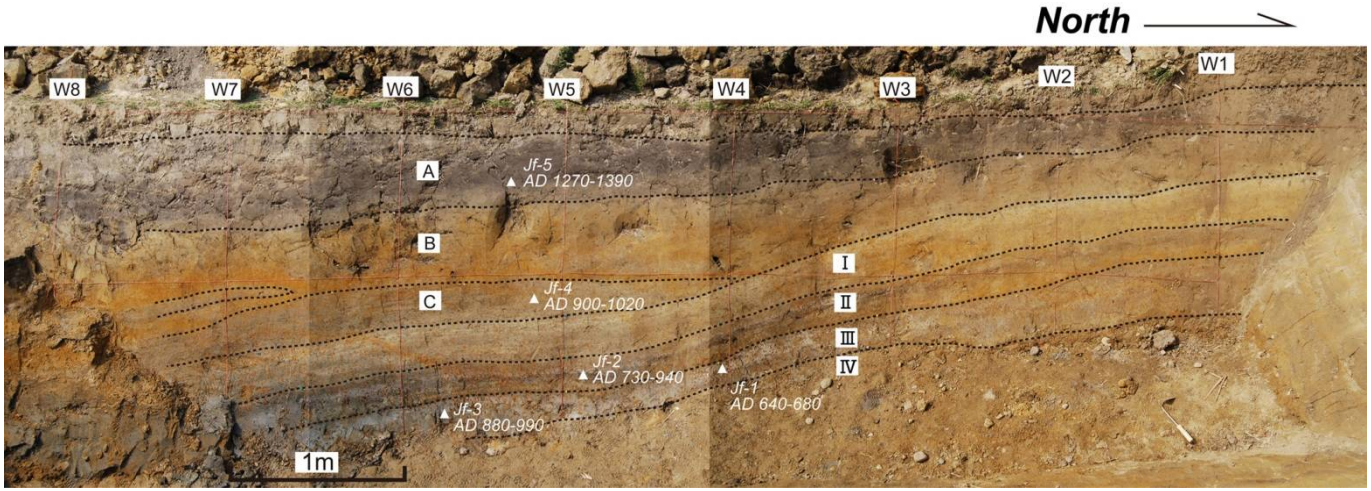

Figure 28. Mosaic photo of the west wall at Jaflong 1 trench site

Table 2　Result of ^{14}C dating at Jaflong trench site

Trench	Unit	Sample number	Laboratory number	Method	Material	Measured radiocarbon age (yBP)	δ 13C (permil)	Conventional radiocarbon age (yBP)	Calibrated Calender years (2 sigma)
Jaflong	A	Jaf-5	Beta-319595	AMS	organic sediment	540 ± 30	-16.3	680 ± 30	AD 1270 to 1390
	B	Jaf 2-5	Beta-319587	AMS	organic sediment	1120 ± 30	-20.9	1190 ± 30	AD 730 to 940
	C	Jaf 2-6	Beta-319588	AMS	organic sediment	1130 ± 30	-22.6	1170 ± 30	AD 780 to 970
		Jaf-4	Beta-319594	AMS	organic sediment	1030 ± 30	-22.8	1070 ± 30	AD 900 to 1020
		Jaf 2-8	Beta-319590	AMS	organic sediment	1050 ± 30	-24.5	1060 ± 30	AD 900 to 1020
		Jaf 2-7	Beta-319589	AMS	charred material	1110 ± 30	-26.7	1080 ± 30	AD 890 to 1020
	Ⅰ								
	Ⅱ	Jaf-2	Beta-319592	AMS	organic sediment	1160 ± 30	-23.3	1190 ± 30	AD 730 to 940
		Jaf 2-2	Beta-319584	AMS	organic sediment	1110 ± 30	-19.7	1200 ± 30	AD 720 to 890
		Jaf 2-4	Beta-319586	AMS	organic sediment	1180 ± 30	-23.7	1200 ± 30	AD 720 to 890
		Jaf 2-1	Beta-319583	AMS	wood	1090 ± 30	-24.8	1090 ± 30	AD 890 to 1020
	Ⅲ	Jaf-3	Beta-319593	AMS	charred material	1150 ± 30	-27.1	1120 ± 30	AD 880 to 990
		Jaf-1	Beta-319591	AMS	organic sediment	1330 ± 30	-22.7	1370 ± 30	AD 640 to 680
		Jaf 2-3	Beta-319585	AMS	organic sediment	1540 ± 30	-19.8	1630 ± 30	AD 380 to 530

Figure 29a. Photo of the west wall at Jaflong 1 trench site. The whitish layer is unit I which shows a warping structure.

Figure 29b. Photo of the east wall. The whitish layer shows a warping structure.

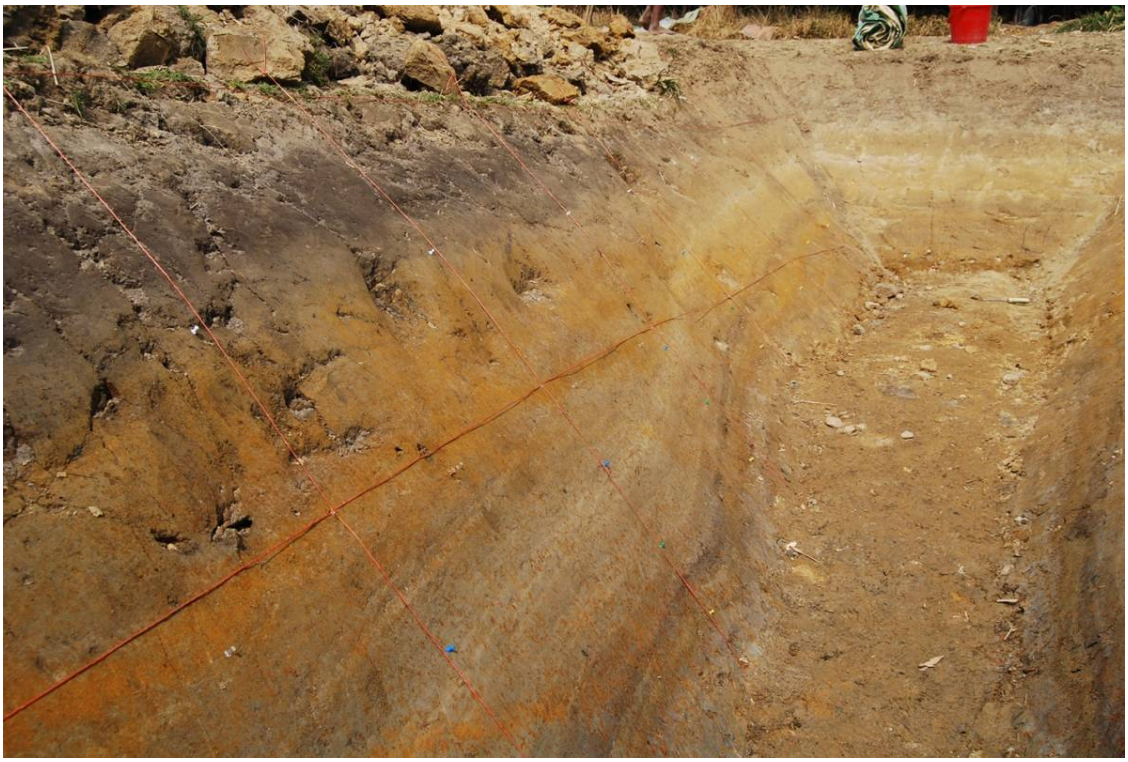

Figure 29c The thread represents horizontal and vertical lines with intervals of 1 m.

Figure 29d. The whitish layer is inclined to the south with ~10°.

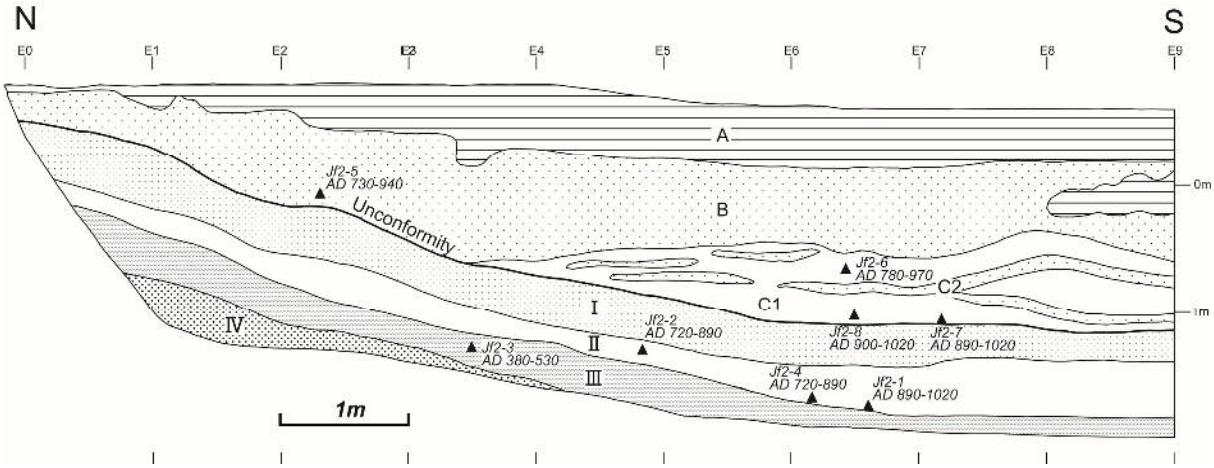

Figure 30. Log of the east wall at Jaflong 2 trench site

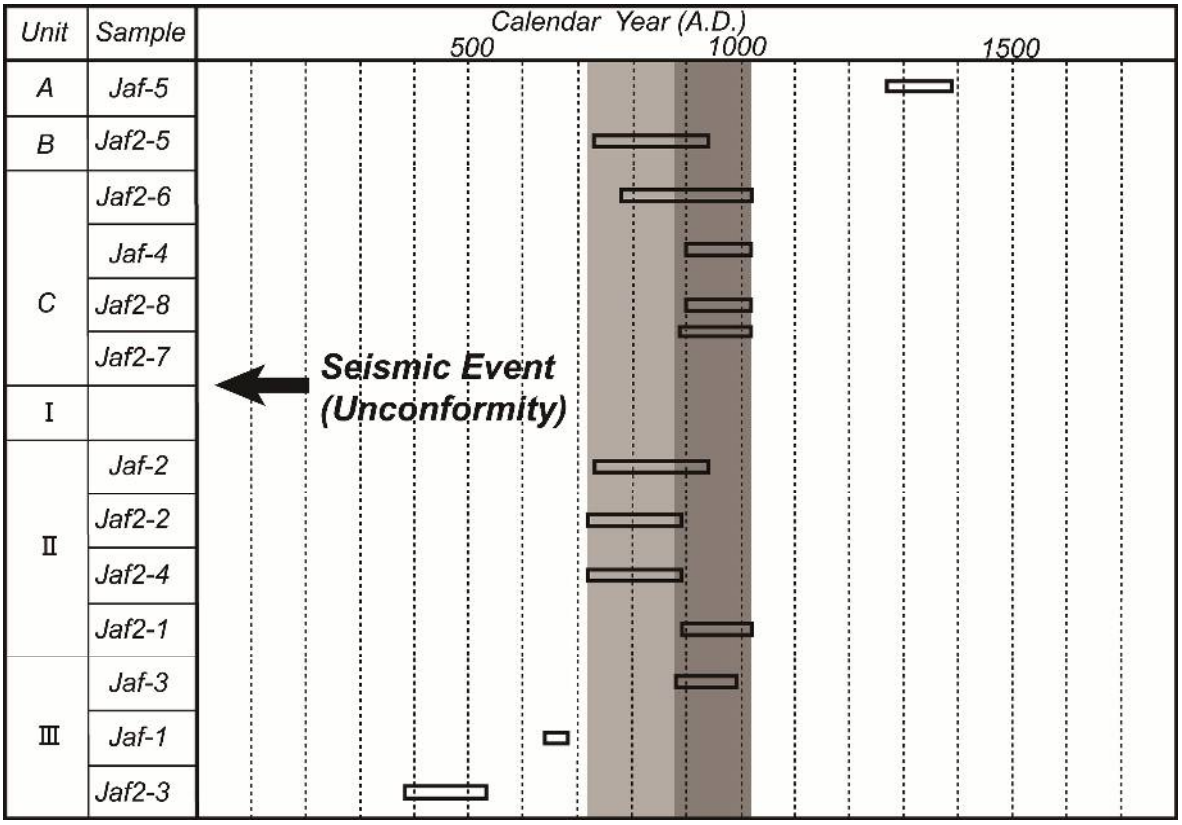

Figure 31. Timing of the seismic event at Jaflong trench site. It is dated to AD 720-1020. If younger ages are adopted, the timing of the seismic event is limited to AD 880-1020.

4.2 Tripura segment

We could not identify any active fault related to the Tripura segment, though the trench investigation was carried out at three sites of Shahzibazar, Kasba, and Comilla Hill. As typically shown at Kasba (Figs. 17 and 18), the fault scarp is eroded and shifted. Instead, a crater for a large paleo-liquefaction and a lateral flow were found at Kasba and Comilla Hill, respectively. These are thought to be structures which were made up by the strong seismic motion of a large paleo-earthquake. The timing of paleo-earthquake was inferred from the crater and lateral flow.

1) Shahzibazar, Habiganj

The trench investigation was carried out across the wide warping scarp (Fig. 16). The crater was found in the trench, though no active fault and deformation were identified.

The crater is shown in Fig. 32. The top of the crater is ~3 m wide. The timing of the charcoal in the silt layer, which is intruded by the liquefied sand, is dated to 1120-910 BC (Hob-C). The charcoal in the deposit, which covers the crater, is dated to 1260-1000 BC (Hob-D). The deposit overlying the crater shows older age than the silt intruded by the liquefied sand. It is thought that the sample of Hob-D was reworked from the older deposit. It is inferred that the seismic event which created the crater has occurred after 1120-910 BC.

2) Kasba

As shown in Figs. 17 and 18, the trench was excavated at the western edge of the back-tilted terrace. Although no active fault was identified in the trench, the layers were gently tilted towards the east as well as the terrace surface. The scarp at the western edge of the terrace is assumed to be an eroded one. The fault may be located more west and shifted to the present place by the fluvial erosion.

We collected three samples of wood fragments from the same layer in the trench and performed the radiocarbon dating. The samples of Ks-1, Ks-2, and Ks-3 are dated to 2920 -2880 BC, 5220-5040 BC, and 785-515 BC, respectively. The dating result varies widely. However, there is no mixing of wood roots into the samples (Geo-Science Laboratory). It is assumed that older wood fragments are reworked from older layers. The terrace at Kasba is thought to be uplifted after 785-515 BC.

The shallow seismic reflection survey is planned at Kasba. The trench investigation will be again tried after the shallow seismic reflection survey.

3) Comilla Hill

The trench investigation was carried out at the western edge of the Comilla Hill (Fig. 20b). The log of north wall and its mosaic photo are shown in Figs. 33a and 33b, respectively. The result of ^{14}C dating is shown in Table 3.

Stratigraphy identified in the trench

The stratigraphy in the trench is divided into units A to E. Units A, B, C, and E are inferred to be channel deposits. Unit D is inferred to be a swamp deposit.

Unit A: Yellowish brown sandy silt.

Unit B: Mainly gray fine sand. Weakly stratified alternation of silt and fine sand is partly recognized.

Unit C: Gray silt.

Unit D: Blackish peaty clay.

Unit E: Gray alternation of silt and fine sand.

Lateral flow

It seems that Unit E has flowed towards the west and has been deformed by the paleo-liquefaction caused by the strong ground motion. The depression between horizontal markers N4 and N5 is inferred to be a crack which was created by lateral flow of unit E. It is thought that the ground water has sprung by paleo-liquefaction and lateral flow during the large earthquake, and the ground around the trench site has changed into a swamp environment, and unit D has been deposited. The seismic event which has caused a lateral flow is inferred after the deposition of unit E and before the deposition of unit D.

Timing of seismic event

While the samples Co-3, 4, and 5 of unit D show similar age of 810-400 BC, the sample Co-6 of unit E shows a younger age of AD 20-130 (Fig. 33a and Table 3). During the trench investigation, we thought that the sample Co-6 is plant fragments. But, Geo-Science laboratory suggested that it may be a wood root and show a young age. The samples collected from unit D represent right age. The seismic event is inferred to have occurred before 810-400 BC from the radiocarbon age of unit D.

Figure 32. A crater for a large paleo-liquefaction identified at Shahzibazar, Habiganj

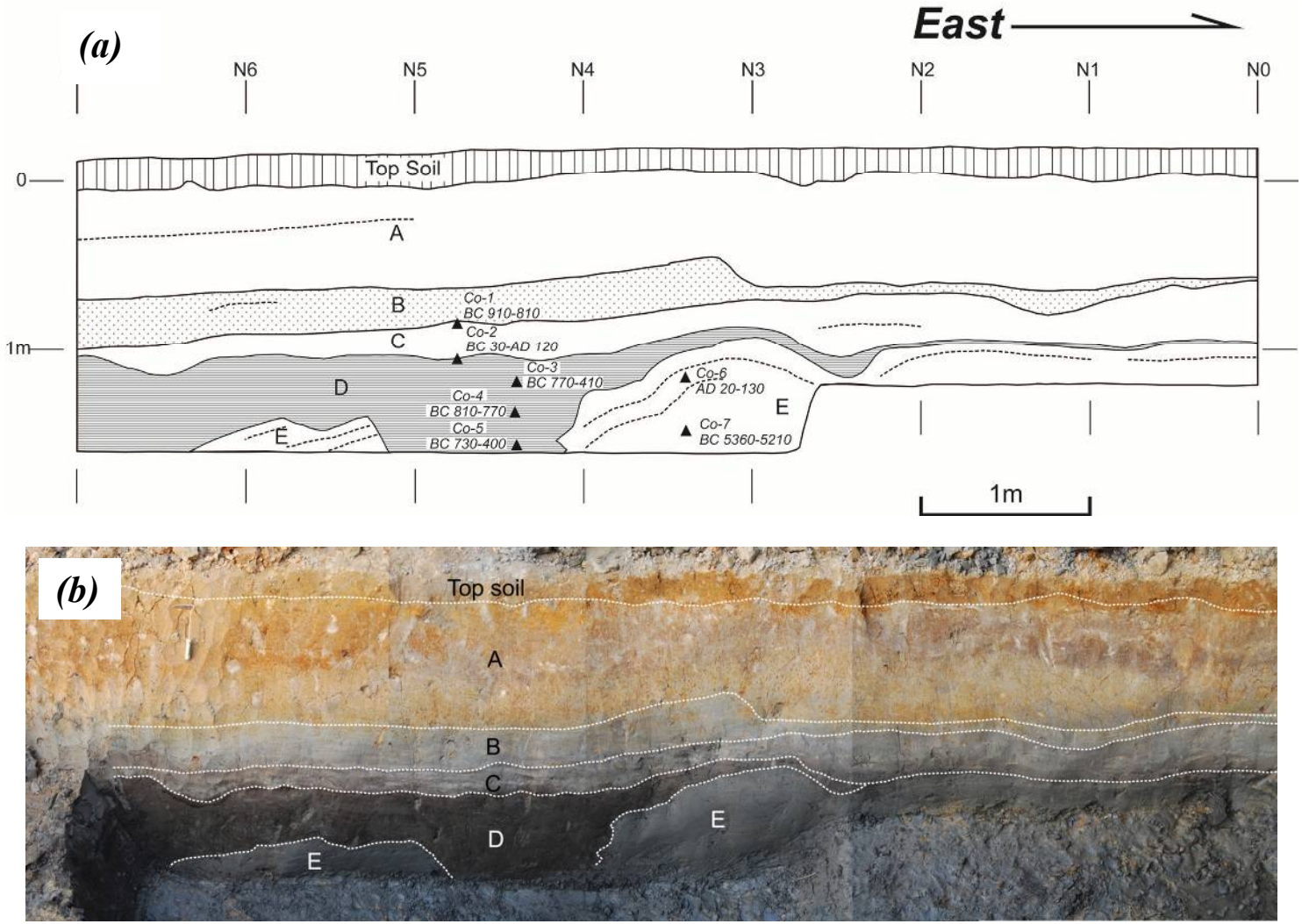

Fig. 33. (a): Log of north wall at Comilla Hill trench site. (b): Mosaic photo of north wall.

Table 3 Result of ^{14}C dating

Trench	Unit	Sample number	Laboratory number	Method	Material	Measured radiocarbon age (yBP)	δ 13C (permil)	Conventional radiocarbon age (yBP)	Calibrated Calender years (2 sigma)
Comilla Hill	C	Co-1	319599	AMS	organic sediment	2700 ± 30	−24.3	2710 ± 30	BC 910 to 810
		Co-2	319600	AMS	organic sediment	1980 ± 30	−26.8	1950 ± 30	BC 30 to AD 120
	D	Co-3	319601	AMS	organic sediment	2490 ± 30	−25.9	2480 ± 30	BC 770 to 410
		Co-4	319602	AMS	organic sediment	2620 ± 30	−25.5	2610 ± 30	BC 810 to 770
		Co-5	319603	AMS	organic sediment	2420 ± 30	−25.5	2410 ± 30	BC 730 to 400
	E	Co-6	319604	AMS	plant material	1940 ± 30	−26.2	1920 ± 30	AD 20 to 130
		Co-7	319605	AMS	organic sediment	6260 ± 40	−22.4	6300 ± 40	BC 5360 to 5210

5. Evaluation of active faults

5.1 Faulting history of active faults

To evaluate the risk of earthquake occurrence, it is necessary to know the faulting history of active faults based on the paleo-seismological studies. However, the paleo-seimological studies of Bangladesh are still in infancy. In this chapter, the seismic risk of active faults will be evaluated from present data.

1) Dauki fault

The seismic events in AD 880-1020 and in AD 1548 are inferred from the trench investigation at Jaflong and Gabrakhari, respectively. We suggest that the 1548 earthquake has been caused by the rupture of the Dauki fault, while Bilham and Hough (2006) and Steckler et al. (2008) suggested the Tripura segment as a seismic source from the damages of Sylhet and Chittagong. As mentioned by Steckler et al. (2008), it is contradictory that there is no record of the damage in Dhaka or nearby Sonargaon, the capital of Bangladesh at the time. Also there is no paleo-seismological evidence that the Tripura segment has ruptured in AD 1548.

Although the seismic event in 1897 could not be identified by the trench investigation across the Dauki fault, it is inferred that the Dauki fault is a seismic source of the 1897 earthquake from the hat-shaped high intensity distribution (Oldham, 1899).

Sukhija et al. (1999) carried out the paleo-liquefaction study along the Krishnai River and Dudhnai River. They suggested twice paleo-liquefaction events except the 1897 earthquake, namely the seismic events in 1100 ± 150 years BP and in 1500 ± 150 years BP. Rajendran et al. (2004) reexamined the data of radiocarbon age after Sukhija et al. (1999), and modified these ages into calendar year in AD 700-1050 and AD 1450-1650. The time of these paleo-liquefaction events corresponds to that of the seismic events identified in the trench at Jaflong and Gabrakhari. The Shillong Plateau has been strongly shaken by the rupture of the Dauki fault and paleo-liquefactions have been caused by the shaking, since the Dauki fault dips beneath the Shillong Plateau.

The Dauki fault is inferred to have ruptured historically three times in AD 1897, AD 1548, and AD 880-1020. The recurrence interval is 350 to 650 years, and the elapse time since the 1897 earthquake is 116 years.

2) Tripura segment

Bilham and Hough (2006) and Steckler et al. (2008) suggested that the Tripura segment

has ruptured in AD 1548, while there are no paleo-seismological evidences.

According to our paleo-seismological studies, the crater at Shahzibazar, Habigonj was created after 1120-910 BC. The back-tilted terrace at Kasba may have been uplifted after 785-515 BC, and the lateral flow at the western edge of the Comilla Hill was created before 810-400 BC. From these paleo-seismological data, the Tripura segment may have ruptured in 1120-400 BC.

The slip rate of the Tripura segment is inferred to be ~5 mm/year from GPS data by Dr. S. H. Akhter. It is significantly small in comparison with 23 mm/year of the Arakan segment. If it is right, the Tripura segment may have a long recurrence interval of several thousands.

The paleo-seismological studies on the Tripura segment are issues in future. In this report, the timing of the latest event of the Tripura segment is suggested to be 1120-400 BC. The recurrence interval is assumed to be 2000 years.

3) Arakan segment

According to the studies of the uplifted marine terraces off Myanmar (Aung et al., 2008; Shishikura et al., 2009), the Arakan segment has ruptured in AD 1762, and the recurrence interval of the 1762-type large earthquake is ~900 years. However, EOS draft report demonstrates that uplifted events are more frequent than this, which implies that large earthquakes are also more frequent (unpublished data). The 1762-type earthquake with the magnitude of ~Mw 8.5 has a long recurrence interval of ~900 years. However, another-type earthquake, the magnitude of which is smaller than the 1762-type, may occur between the 1762-type large earthquakes. In this case, the recurrence interval of the Arakan segment may be 300 or 450 years.

4) Active faults within Chittagon-Tripura Fold Belt (CTFB)

There is no data on the faulting history of active faults within the CTFB. While the 1822 earthquake and the 1918 Srimongal earthquake may be ascribed to the ruptures of the active faults within the CTFB, it is unknown whether these are characteristic earthquakes or not. If the earthquakes within the CTFB are estimated as floating earthquakes, the recurrence interval is ~100 years.

5) Madhupur blind fault

It is believed that the 1885 Bengal earthquake may have been caused by the rupture of the Madhupur blind fault. However, there is no paleo-seismological evidence. The Madhupur blind fault may have a long recurrence interval of several thousands, since it is an intra-plate

active fault.

5.2 Probabilistic analysis

The recurrence interval of earthquake shows probability density function (Working Group on California Earthquake Probabilities, 1990). The conditional probability in time interval ΔT, given the elapsed time since the latest seismic event is Te, is shown in the ratio of the area "A" to the area "A + B" (Fig. 34).

The 50 years probability of each fault is shown in Table 4. The Dauki fault shows a relatively high probability with 7.7 %.

The Tripura segment shows a relatively low probability of 5.1 %, although the elapsed time exceeds the recurrence period by 400 years. If the recurrence interval is long with several thousands, the probability is not so high, since the area "A" is small in comparison with the area "A + B" (Fig. 34).

We considered three cases on the Arakan segment. If the recurrence interval is 900 years, the 50 years probability is low with 1.2 %. However, if one time another-type earthquake occurs between the 1762-type large earthquakes, the 50 years probability is 13.4 %. If twice another-type earthquakes occur between the 1762-type large earthquakes, the 50 years probability is 26.9 %. It is thought that if another-type earthquakes occur between the 1762-type large earthquakes, the 50 years probability of the Arakan segment may be high, while the probability of the 1762-type large earthquake is low.

In the present conditions, it is difficult to estimate the 50 years probability of each active fault within the CTFB. If the earthquakes within the CTFB are estimated as floating earthquakes, the recurrence interval is 100 years and the latest event is the 1918 Srimongal earthquake, and the 50 years probability is estimated to be 64.9 %. The probability of the earthquake occurrence with the magnitude as large as the 1918 Srimongal earthquake is very high.

The recurrence interval of the Madhupur blind fault is unknown. If the latest seismic event has occurred in AD 1885 and its recurrence interval is 2000 years for an intra-plate active fault, the 50 years probability is 0 %.

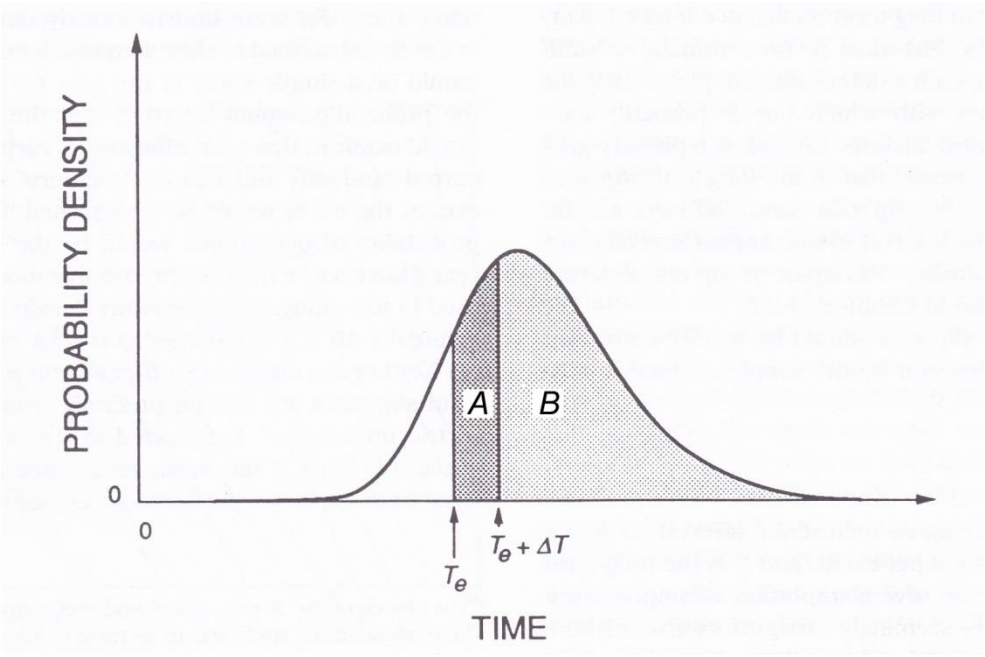

Figure 34. Probability density function for earthquake recurrence. Te: elapsed time since the latest seismic event. ΔT: time interval to calculate the probability (50 years). The conditional probability in time interval ΔT, given the elapsed time since the latest seismic event is Te, is the ratio of the area "A" to the area "A + B". From Working Group on California Earthquake probabilities (1990). Extracted from the figure after Yeats et al. (1997).

Table 4　50 years probability of each active fault

Fault		Events	Recurrence interval (years)	Elapsed time (years)	50 years probability (%)
Dauki fault		AD 1897	350	116	7.7
		AD 1548			
		AD 880–1020			
Indian/Burman plate boundary fault	Tripura segment	BC 1120–400?	2000?	2400?	5.1
	Arakan segment	AD 1762	900	251	1.2
			450	251	13.4
			300	251	26.9
Active faults within the CTFB (Floating earthquake)		AD 1822	100	95	64.9
		AD 1918			
Madhupur blind fault		AD 1885?	2000?	128	0.0

5.3 Fault parameters

The seismic moment "M_0" is calculated from the rupture area "RA" and average displacement "D", and the magnitude "Mw" is estimated from "M_0" (refer the bottom of Table 5). The average displacement "D" is inferred from slip rate of GPS data and recurrence interval.

The fault parameters of each fault are shown in Table 5.

The shortening across the Dauki fault is estimated to be 7 mm/year from GPS data. The slip rate along the fault, if the fault dip is 45°, is estimated to be ~10 mm/year, and the average displacement is estimated to be 3.5 m with the recurrence interval of 350 years. In this case, the magnitude of the Dauki fault is Mw 8.0. It corresponds to the magnitude inferred from the damage distribution of the historical record.

The slip rate (shortening) of the Tripura segment is estimated to be 5 mm/year from GPS data. If the recurrence interval is 2000 years, the average displacement is estimated to be 10 m, and the magnitude is inferred to be Mw 8.9.

The slip rate of the Arakan segment is 23 mm/year from GPS data. The average displacement is varied by the recurrence interval, and the magnitude is inferred to be Mw 8.9-Mw 8.6. However, another-type earthquakes, which occur between the 1762-type large earthquakes, may have smaller rupture area than the 1762-type, since a part of the segment ruptures. In this case, the magnitude is smaller than that shown in Table 5.

If the earthquakes within the CTFB are regarded as floating earthquakes, the magnitude Mw will be inferred from surface rupture length (Wells and Coppersmith, 1994). The magnitude of the earthquakes within the CTFB is estimated to be Mw 7.2-6.6.

If the slip rate of the Madhupur blind fault is 2 mm/year, the average displacement is estimated to be 4 m with the recurrence interval of 2000 years. The magnitude is suggested to be Mw 7.6.

Table 5　Parameters of active faults

Fault		Length (km)	Dip (degree)	Depth (km)	Width (km)	Rupture area RA (km^2)	Slip rate (mm/year)	Recurrence interval (years)	Avarage displacement D (m)	Magnitude Mw
Dauki fault		260	45	35	49	12740	10	350	3.5	8.0[1)]
Indian / Burman plate boundary fault	Tripura segment	250	5	30	340	85000	5	2000	10.0	8.9[1)]
	Arakan segment	440	16	30	108	47520	23	900	20.0	8.9[1)]
								450	10.0	8.7[1)]
								300	6.9	8.6[1)]
Active faults within CTFB (Floatihg earthquakes)		20-60	-	-	-	-	-	-	-	7.2-6.6[2)]
Madhupur blind fault		50	45	30	42	2100	2	2000	4.0	7.6[1)]

1) $M_0 = \mu * D * RA$ (Hanks and Kanamori, 1979)

M_0: seismic moment, μ : shear modulus ($3*10^{11}$), D: average displacement, RA: rupture area

Mw = 2/3 * log Mo − 10.7 (Hanks and Kanamori, 1979)

2) Mw=5.0 + 1.22 * log (SRL) (Wells and Coppersmith, 1994)

SRL: surface rupture length (km)

6. Issues in future

There is less information on the active faults, since the paleo-seismological study in Bangladesh is in infancy. It is indispensable to continue the paleo-seismological study based on trench investigation. The issues in future are as follows:

1) Paleo-seismological investigation of each active fault

On the Dauki fault, two paleo-earthquakes in historical time are revealed by the trench investigation at Gabrakhari and Jaflong. However, there is no definitive evidence that the Dauki fault has ruptured during the 1897 earthquake. Gabrakhari and Jaflong are located on the west and the east of the Dauki fault, respectively. The detailed field survey is not still carried out in the central part of the Dauki fault. It is desirable to carry out the tectonic-geomorphic investigation and trench investigation in the central part of the Dauki fault. The trench investigation should be carried out after the shallow seismic reflection survey, since the geomorphology such as fault scarp or warping scarp is modified by agriculture.

No active fault of the Tripura segment is identified. Judging from our tectonic-geomorphic investigation, the fault scarp along the Tripura segment is eroded. After the shallow seismic reflection survey, trench investigation at Kasba and Comilla Hill should be tried again.

On the Madhupur blind fault, shallow and deep seismic reflection surveys are necessary to detect a blind fault, and drilling survey and trench investigation will be tried if possible.

2) Deep seismic reflection survey across the Tripura segment

There are two suggestions on the fault trace of the Tripura segment. One is the deformation front, and another is active faults on the western margin of the Chittagong-Tripura Fold belt (CTFB). It is essential to clarify which is a main plate boundary. Even if the deformation front is a main plate boundary, another large active fault may be present on the western margin of the CTFB. The deep seismic reflection survey from the western margin of the CTFB to the Padma River is desirable. If the structure of the CTFB to the deformation front is revealed, the location of the main plate boundary will be revealed.

References

Abe, K., 1994, Instrumental magnitudes of historical earthquakes, 1892 to 1898. Bulletin of the Seismological Society of America, **84**, 415-425.

Alam M. K., A. K. M. S. Hasan, M. R. Khan, and J. W. Whitney, 1990, 1: 1000,000 Geological map of Bangladesh.

Ambraseys, N. N., and J. Douglas, 2004, Magnitude calibration of north Indian earthquakes. *Geophys. J. Int.*, **159**, 165 – 206

Aung, T. T., K. Satake, Y. Okamura, M. Shishikura, W.Swe, H. Saw, T. L. Swe, S. H. Tun, and T. Aung, 2008, Geologic evidence for three great earthquakes in the past 3400 years off Myanmar. *Journal of Earthquake and Tsunami*, **2**, 259-265.

Bilham, R. and P. England, 2001, Plateau pop-up during the great 1897 Assam earthquake. *Nature*, **410**, 806-809.

Bilham, R., and S. Hough, 2006, Future Earthquakes on the Inidan Subcontinent: Inevitable Hazard, Preventable Risk. *South Asian Journal*, **12**, 1-9.

Halsted, E. P., 1843, Report on the Island of Cheduba. *J. Asian Soc. Bengal*, **114**, 349-446.

Hanks, T. C. and H. Kanamori, 1979, A moment-magnitude scale. *Jour. Geophys. Res.*, **84**, 2348-50.

Iyengar, R. N., D. Sharma, and J. M. Siddiqui, 1999, Earthquake history of India in medieval times. *Indian J. Hist. Sci.*, **34**, 181 – 237.

Johnson, S. Y. and A. M. Nur Alam, 1991, Sedimentation and tectonics of the Sylhet trough, Bangladesh. *Geol. Soc. Am. Bull.*, **103**, 1513-1527.

Martin, S., and W. Szeliga, 2010, A catalog of felt intensity data for 589 earthquakes in India, 1636–2008. *Bull. Seismol. Soc. Am.* **100**, no. 2, 562–569.

Maurin, T. and C. Rangin, 2009, Structure and kinematics of the Indo‐Burmese Wedge: Recent and fast growth of the outer wedge. *Tectonics*, **28**, TC2010, doi:10.1029/2008TC002276.

Middlemiss, C.S., 1885, Report on the Bengal Earthquake of 14th July 1885, Records of the Geological Survey of India, Vol. XVIII, pt. 4, 200-221.

Morino, M., A. S. M. M. Kamal, D. Muslim, R. Md. E. Ali, M. A. Kamal, Md. Z. Rahman, and F. Kaneko, 2011, Seismic Event of the Dauki Fault in 16th Century Confirmed by Trench Investigation at Gabrakhari Village, Haluaghat, Mymensingh, Bangladesh. *Journal of Asian Earth Sciences*, **42**, 492-498. doi: 10.1016/j.jseaes. 2011.05.002

Morino, M. and A. S. M. M. Kamal, 2012, Flexure structure of the Dauki Fault and its

Geomorphic Features at Jaflong, the North of Sylhet, Bangladesh. *Japanese Society for Active Fault Studies, fall meeting 2012*, O-11 (in Japanese).

Nakata, T., 1975, On Quaternary tectonic around the Himalayas. *Science Report Tohoku University. 7th ser*. (Geography), **25**, 111-118.

Nakata, T., 1989, Active faults of the Himalaya of India and Nepal. Geol. Soc. America Spec. Paper **232**, 243-264.

Narula, R.L., S. K. Acharrya, J. Banerjee, (Eds.), 2000, Seismotectonic atlas of India and its environs. Geological Survey of India, Kolkats, 43p.

Oldham, T., 1883, Catalogue of Indian Earthquakes. Memoirs Geological Survey of India, **19**(3), pp.170.

Oldham, R. D., 1899, Report of the great earthquake of 12th June 1897. *Mem. Geol. Surv. India.*, **29**, 379p (Reprinted by Geol. Surv. of India, Calcutta, 1981).

Rahman, M. A., M. A. Mannan, H. Richard Blank, M. Dean Kleinkopf, and Robert P. Kucks, 1990, Bouguer gravity anomaly map of Bangladesh. Geological survey of Bangladesh.

Rajendran, C. P., K. Rajendran, B. P. Duarah, S. Baruah, and A. Earnest, 2004, Interpreting the style of faulting and paleoseismicity associated with the 1897 Shillong, northeast India, earthquake: Implications for regional tectonism. *Tectonics*, **23**, TC4009, doi: 10.1029/2003TC001605.

Richter, C. F., 1958, Elementary Seismology. W. H. Freeman, San Francisco.

Shishikura, M., Y. Okamura, K. Satake, S. Fujino, T. T. Aung, W. Swe, W. Naing, H. Soe, S. T. Tun, T. L. Swe., and T. Aung. (2009). Geomorphological evidence of great Holocene earthquakes off western Myanmar. Proceedings of the international workshop on Tsunami and storm surge hazard assessment and management for Bangladesh, 22

Steckler, M.S., S.H. Akhter, and L. Seeber, 2008, Collision of the Ganges–Brahmaputra Delta with the Burma Arc: implications for earthquake hazard. *Earth planet Sci. Lett.*, **273**, 367–378.

Sukhija, B. S., M. N. Rao, D. V. Reddy, P. Nagabhushanam, S. Hussain, R. K. Chadha and H. K. Gupta, 1999, Timing and return period of major paleoseismic events in the Shillong Plateau, India. *Tectonophysics*, **308**, 53-65.

Stuart, M., 1920, The Srimangal earthquake of 8th July 1918. Memoirs of the Geological Survey of India, **46** (1).

Szeliga, W., S. Hough, S. Martin and R. Bilham, 2010, Intensity, magnitude, location and attenuation in India for felt earthquakes since 1762. Bull. *Seism. Soc. Amer.* **100**, 2, 570-584

Wells, D. L. and K. J. Coppersmith, 1994, New Empirical Relationships among Magnitude,

Rupture Length, Rupture Width, Rupture Area, and Surface Displacement. *Bull. Seismol. Soc. Am.*, **84**, 974-1002.

Working Group on California Earthquake Probabilities (WGCEP), 1990, Probabilities of large earthquakes in the San Francisco Bay region, California. U. S. Geol. Survey Circular, 1053, 51p.

Yeats, R. S., K. Sieh, and C. R. Allen, 1997, The geology of earthquakes. Oxford University Press, 568p.